AD_____

TECHNICAL REPORT NO. 3

PROJECT ZULU II - PHASE I
SINGLE-CHARGE CALIBRATION SERIES

SP4 W. W. JOHNSON
1LT D. L. NELSON

U. S. Army Engineer Nuclear Cratering Group
Lawrence Radiation Laboratory
Livermore, California

November 1968

78

TECHNICAL REPORT NO. 3

PROJECT ZULU II - PHASE I
SINGLE-CHARGE CALIBRATION SERIES

SP4 W. W. JOHNSON
1LT D. L. NELSON

U. S. Army Engineer Nuclear Cratering Group
Lawrence Radiation Laboratory
Livermore, California

November 1968

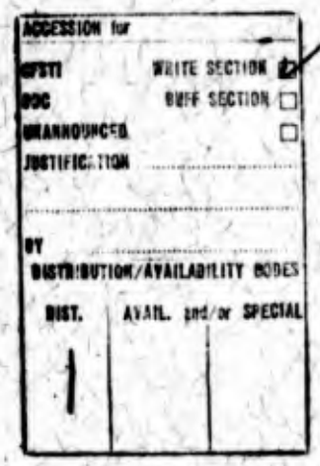

Destroy this report when no longer needed.
Do not return it to the originator.

The findings in this report are not to be construed as an official Department of the Army position unless so designated by other authorized documents.

Printed in USA. Available from Defense Documentation Center,
Cameron Station, Alexandria, Virginia 22314 or
Clearinghouse for Federal Scientific and Technical
Information, National Bureau of Standards,
U. S. Department of Commerce,
Springfield, Virginia 22151.

Price: Printed copy $3.00; Microfiche $0.65

PREFACE

This report represents the compilation of working notes, technical memoranda, and experimental results concerning Phase I of Project ZULU II, the single-charge calibration series. Project ZULU II was initiated by Major B. C. Hughes and continued by Major R. H. Benfer. Others closely associated with the program were: Captain D. D. DeFord, Captain W. G. Christopher, and First Lieutenant K. L. Larner.

The Directors of the Nuclear Cratering Group during the execution of this project and the preparation of this report were Lieutenant Colonel Walter J. Slazak and Lieutenant Colonel Bernard C. Hughes.

ABSTRACT

Phase I of Project ZULU II was a laboratory-scale crater modeling experimental series consisting of the detonation of forty-two 1-pound C-4 charges in a moist compacted sand. This experimental series was conducted by the U. S. Army Engineer Nuclear Cratering Group (NCG) at the University of California Lawrence Radiation Laboratory's (LRL) High Explosive Test Facility, Site 300, near Livermore, California.

The primary objectives of Phase I of Project ZULU II were: (1) to calibrate the medium with respect to its cratering characteristics; (2) to determine the reproducibility of the crater dimensions; (3) to conduct surface motion studies; and (4) to study ejecta and fallback distribution as well as the nature of the displacements occurring in the near vicinity of the zero point and the rupture zone.

The cratering curves developed from these experimental series showed an optimum depth of burst (DOB) of 1.5 feet and a rapid decrease of apparent crater dimensions until no crater resulted at a DOB greater than approximately 2.1 feet. The data for ten charges detonated at a nominal DOB of two feet resulted in a fractional standard deviation of 6.4% for crater radius and 20.6% for crater depth, the largest deviations observed for any DOB. The detonation of additional one-half-pound and two-pound C-4 single charges showed that cube-root scaling of apparent crater dimensions was applicable at these yields.

The maximum surface ground zero (SGZ) vertical target velocity, V_{SGZ}, was observed to be a function of DOB and conformed to the relationship $V_{SGZ} = 470/DOB^{3.1}$. The resultant velocity, V, of a surface target can be described in terms of DOB and the cosine of the angle between the

vertical and a line drawn through the surface target and the shot point, θ_r. This equation can be expressed as:

$$V = \frac{470 \ \mathrm{Cos}^{3.6} \theta_r}{\mathrm{DOB}^{3.1}}$$

The ejecta pellet studies did not successfully record pre- and postshot locations of the material actually ejected from the crater. Analysis of the ejecta pellets displacement data, however, did indicate that the fallback was composed primarily of material which was originally either directly over the zero point or in close proximity to the apparent crater boundary.

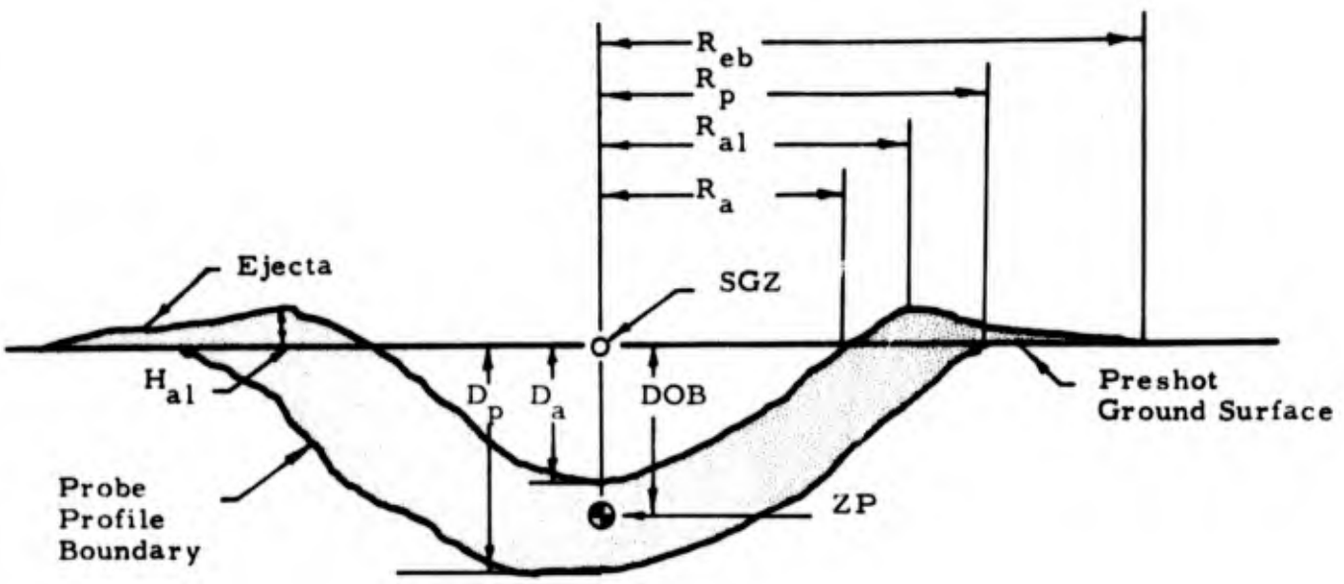

D_a	-	Maximum depth of apparent crater below and normal to the preshot ground surface.
D_p	-	Maximum depth of probe profile below preshot ground surface.
DOB	-	Depth of burial normal to preshot ground surface.
R_a	-	Radius of apparent crater measured at preshot ground surface datum.
R_{al}	-	Radius of apparent lip crest to center of crater.
R_p	-	Radius of probe profile measured on preshot ground surface.
R_{eb}	-	Radius of outer boundary of continuous ejecta.
H_{al}	-	Apparent crater lip crest height above preshot ground surface.
SGZ	-	Surface ground zero.
ZP	-	Zero Point - Effective center of explosion energy.
V_a	-	Volume of apparent crater below preshot ground surface.

SINGLE-CHARGE CRATER NOMENCLATURE

CONTENTS

CONTENTS (Cont.)

LIST OF TABLES

LIST OF FIGURES

LIST OF FIGURES (Cont.)

BLANK PAGE

CHAPTER 1

INTRODUCTION

1.1 PURPOSE

The purpose of Phase I of Project ZULU II was to study the phenomenology of cratering on a laboratory-scale using single one-pound charges of C-4 in a moist, compacted sand medium. Specific objectives of this phase of ZULU II were: (1) to determine the reproducibility of crater dimensions in the modeling medium; (2) to develop cratering curves for apparent crater radius and apparent crater depth as a function of depth of burst; (3) to study the time history of the mound development; (4) to determine the origin of ejecta and fallback material and the displacement of material in the vicinity of the zero point; and (5) to develop improved techniques for conducting cratering modeling experiments in the test facility.

The program was conducted by the U. S. Army Engineer Nuclear Cratering Group (NCG) at the University of California Lawrence Radiation Laboratory's (LRL) High Explosive Test Facility, Site 300, near Livermore, California during the period August, 1965 to October, 1966.

1.2 SCOPE

In order to meet the objectives outlined in the preceding paragraphs, a number of operational methods and technical programs were adopted as standard experimental procedure. The scope of this report and the method of presentation of the experimental findings are primarily based upon the following three main technical programs: (1) crater measurements, (2) surface motion analysis, and (3) studies of ejecta behavior. Chapter II contains a complete description of experimental operations and the technical

programs. This is followed by the experimental results in Chapter III and the analysis of these results in Chapter IV. Chapter V presents the conclusions which are based on this series of experiments.

1.3 BACKGROUND

The decision to use a moist, compacted sand medium for the laboratory-scale crater modeling experiments was based on the results of Project ZULU. Project ZULU tested the suitability of using scalped and remolded desert alluvium as a crater modeling medium. The results of Project ZULU indicated that small changes in moisture and density of the scalped desert alluvium resulted in significant variations in apparent crater dimensions. In order to obtain reproducible crater dimensions, the properties of the alluvium had to be rigidly controlled. For this reason, a well-graded sand with a carefully controlled density was selected as the cratering medium for Project ZULU II.

CHAPTER 2

EXPERIMENTAL PROCEDURE

This chapter describes the test facility, the test medium, the emplacement and detonation of explosive charges, and the procedures used to obtain data relevant to crater measurements, surface motion studies, and ejecta studies.

2.1 DESCRIPTION OF TEST FACILITY

The ZULU II test facility is located at the University of California Lawrence Radiation Laboratory's High Explosive Test Facility, Site 300, near Livermore, California.

The test facility measures 30 x 60 feet (see Figure 2.1) and is filled with moist, compacted sand to a depth of approximately five feet. The facility is equipped with a rolling bridge, used for grading the sand level, and is sheltered by a steel structure with movable canvas roof panels to control the lighting for photography (see Figure 2.2). Enclosures for the high-speed cameras can be placed along one side of the test facility or at either end. The steel frame shelter over the facility has a catwalk that extends down the length of its center. This catwalk is used as a platform for taking aerial stereophotographs of craters.

The Lawrence Radiation Laboratory provided assistance with the necessary labor, materials, and equipment to conduct the experiments. In addition, the Laboratory provided high-explosive technicians to assemble and fire the charges for ZULU II as well as technical assistance for photography, timing, and firing.

2.2 DESCRIPTION OF TEST MEDIUM

2.2.1 Selection of Cratering Medium: A test medium with easily

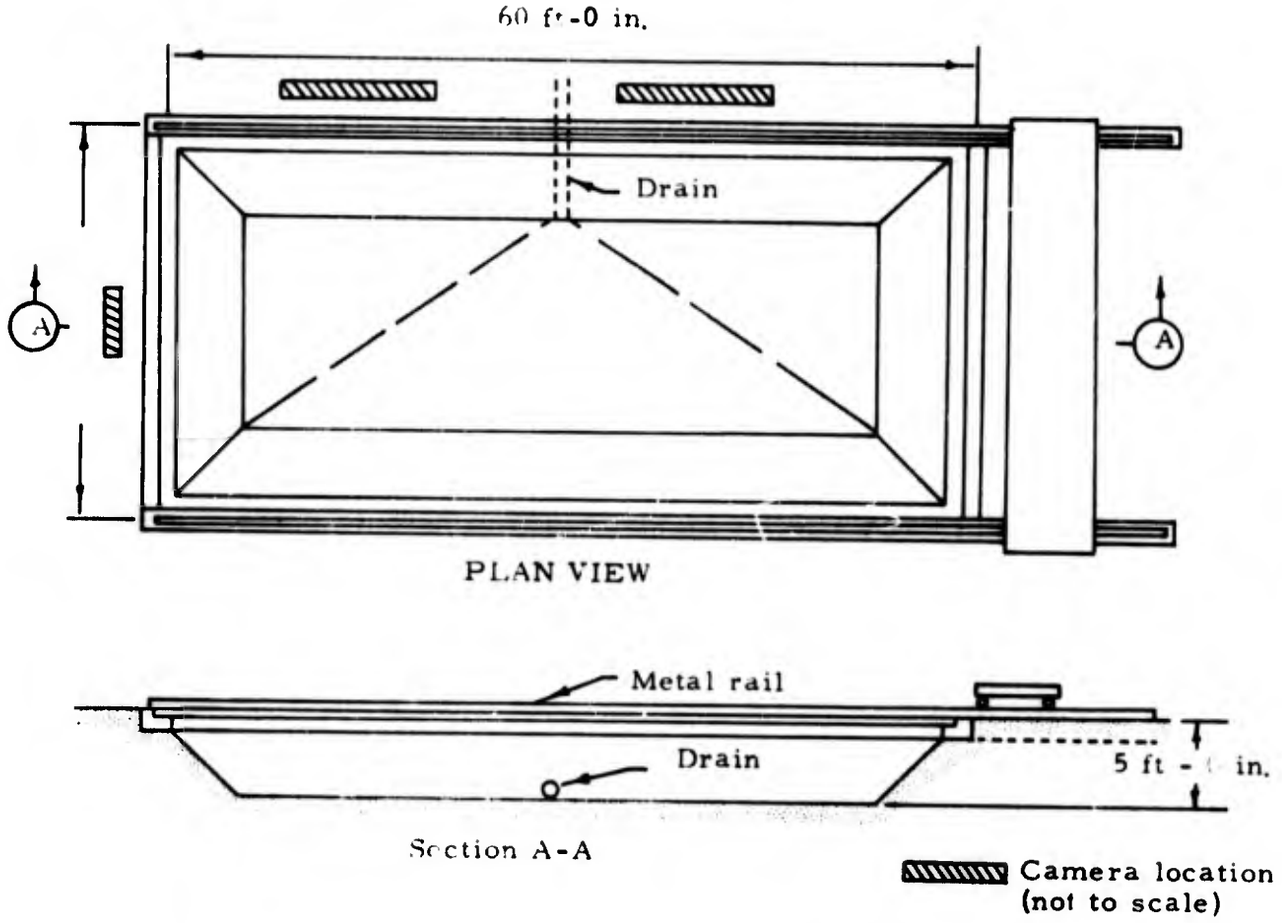

Sketch of test facility

Figure 2.1

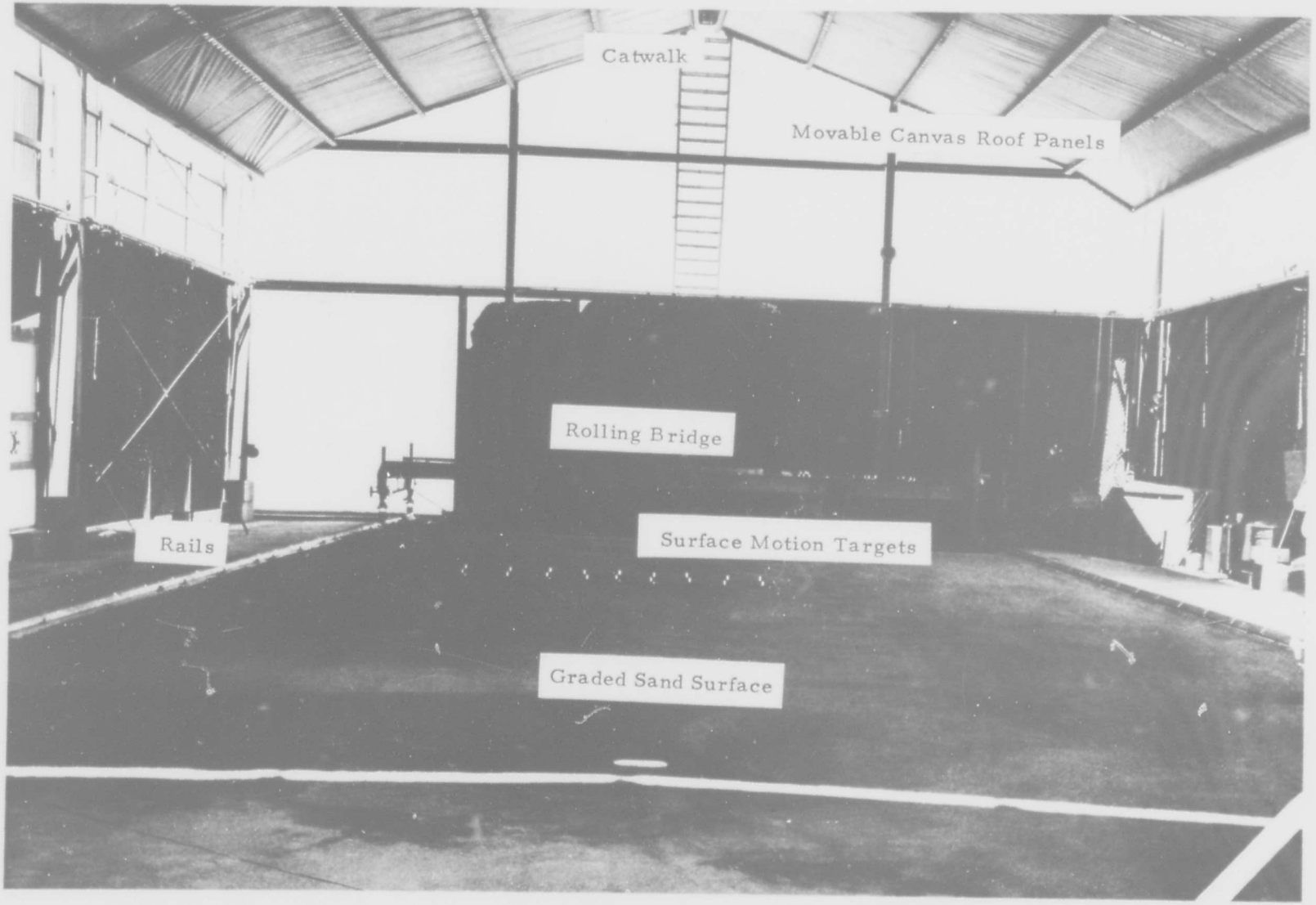

Figure 2.2 Project ZULU II Test Facility Prepared for a Detonation.

controlled properties was necessary for this project. Previous experiments in scalped and remolded alluvium (Project ZULU) indicated that a material with excessive fines was sensitive to changes in moisture content due to the cohesive properties of the fine material.

Extensive laboratory soils tests were performed by the South Pacific Engineer Division Soils Testing Laboratory on four types of sand available locally. The tests included compaction, CBR, gradation, specific gravity, field compaction, Q-type triaxial shear and direct-shear tests. From the results of these tests, a sand with the following gradation characteristics was selected because it exhibited less sensitivity to changes in moisture content than the other sand types:

U. S. Standard Sieve Size	% Passing by weight
# 4	97 - 100
# 8	73 - 88
# 16	53 - 68
# 30	38 - 48
# 50	15 - 25
#100	3 - 10
#200	less than 5%

2.2.2 Quality Control of the Medium. The purpose of the quality control during Project ZULU II was to maintain conditions which would assure reproducibility of crater properties for a given depth of burst. In order to do this, moisture content and density of the sand had to meet specified standards for each detonation.

Tests performed by the South Pacific Division Corps of Engineers Soils Testing Laboratory[2], indicated that 11 passes of a Wacker

Vibratory Compactor over a 7-inch layer of loose sand with a moisture conten between 5 and 6 percent would yield the most consistently reproducible densities. In order to meet these optimum specifications, the following procedure was used for backfilling the pit after each detonation:

1. A tractor, equipped with a front-end loader, filled the scale hopper to the proper batch weight.

2. The scale hopper discharged into a skip-loading concrete mixer.

3. The sand was mixed to the desired moisture content of six percent by measuring the moisture content at intervals during the mixing and adding water as necessary to obtain the desired result.

4. The prepared sand was placed in the pit by a front-end loader.

5. Each lift was emplaced as 7 inches of loose sand, leveled to preset stake elevations, then compacted with 11 passes of a Wacker VPG 160 Vibratory Compactor.

The following tests were performed to assure that this procedure produced the desired results:

1. Moisture tests before and after mixing the sand.

2. In-place density tests.

3. Moisture tests of in-place material taken from shot emplacement holes.

4. Sieve analysis to assure the uniformity of the test material.

Moisture tests performed during the mixing of the sand were made with an Ashworth MC320 Speedy Moisture Meter. Final moisture tests of the in-place sand were made by oven drying selected samples.

Density tests on the in-place material were made with the Reinhart No. 216 Balloon Volumeter. The Reinhart Volumeter uses a balloon filled with water to measure the volume of a small test hole for which the weight of excavated material can be determined to compute the density. During backfill operations, one density test was made for each lift. Postshot density tests were made on a number of single-charge craters by driving thin-walled cylinders of known volume into the sand. The material was then excavated from around the cylinders and the material remaining in the cylinder was weighed to determine its density. (These densities are included in Table 3.1.)

The logarithmic sieve series was used to check the gradation of the sand used on Project ZULU II. These included the Numbers 4, 8, 16, 30, 50, 100, and 200 sieves. The material specifications limited the amount of sand passing the No. 200 sieve to 5 percent or less of the total. Because the amount of sand passing the No. 200 sieve was consistently under 5 percent of the total, the No. 200 sieve was eliminated from the series. Two samples for gradation testing were taken from the material used to fill each hole during the postshot backfill operations.

2.3 DESCRIPTION OF THE EXPLOSIVE CHARGES

Two types of charges were considered for use on Project ZULU II. The first charge considered was an aluminum sphere containing 410 ml of nitromethane and center detonated by a detonator and a 10-gram ball (based on heat of detonation comparison) of C-4. Nitromethane is a liquid explosive and has a TNT equivalence of 1.1, i.e. 1.0 pound of nitromethane is equivalent in yield to 1.1 pounds of TNT. The second charge considered was a one-pound charge of C-4 molded into a thin spherical shell of plastic.

C-4 is a plastic explosive which has a TNT equivalence of 1.3. Exploding bridgewire detonators with PETN booster pellets were used for both explosives.

Both explosives were tested using high-speed photography and three types of detonators (SE-1, EX-3, and EX-12). C-4 was selected as the explosive for the experiment because examination of the high-speed photography revealed that the non-uniform structure of the aluminum nitromethane container significantly deformed the shock wave. The SE-1 type detonator was chosen as the most reliable detonator tested (see Figure 2.3).

2.3.1 Charge Preparation and Emplacement. Surface Ground Zero (SGZ) locations were marked by intersecting taut strings. The emplacement holes were dug to shot depth with a 4-inch hand auger and an auger jig to keep the auger vertically alined.

A tamper which was the same size and shape as the charge was used to establish the final elevations of the emplacement holes. For the first few detonations the elevation of the Zero Point (ZP) was checked with a standard Philadelphia rod set in the bottom of the hole. However, the elevation of the ZP for most of the charges was checked by placing the rod on the tamper before removing it from the hole. The charge position was checked after placing the charge and the hole was carefully backfilled by dropping material into the hole and tamping with a lucite rod.

2.3.2 Firing Equipment and Firing Sequence. The firing equipment used during Phase I of Project ZULU II is a three-channel Capacitor Discharge Unit (CDU) with six points per head. Each point on the CDU is served by a 1 uf capacitor and the unit is set to discharge at 2100 to 2250 volts. The firing cables (designated 31 C PT) were coaxial cables with type 31

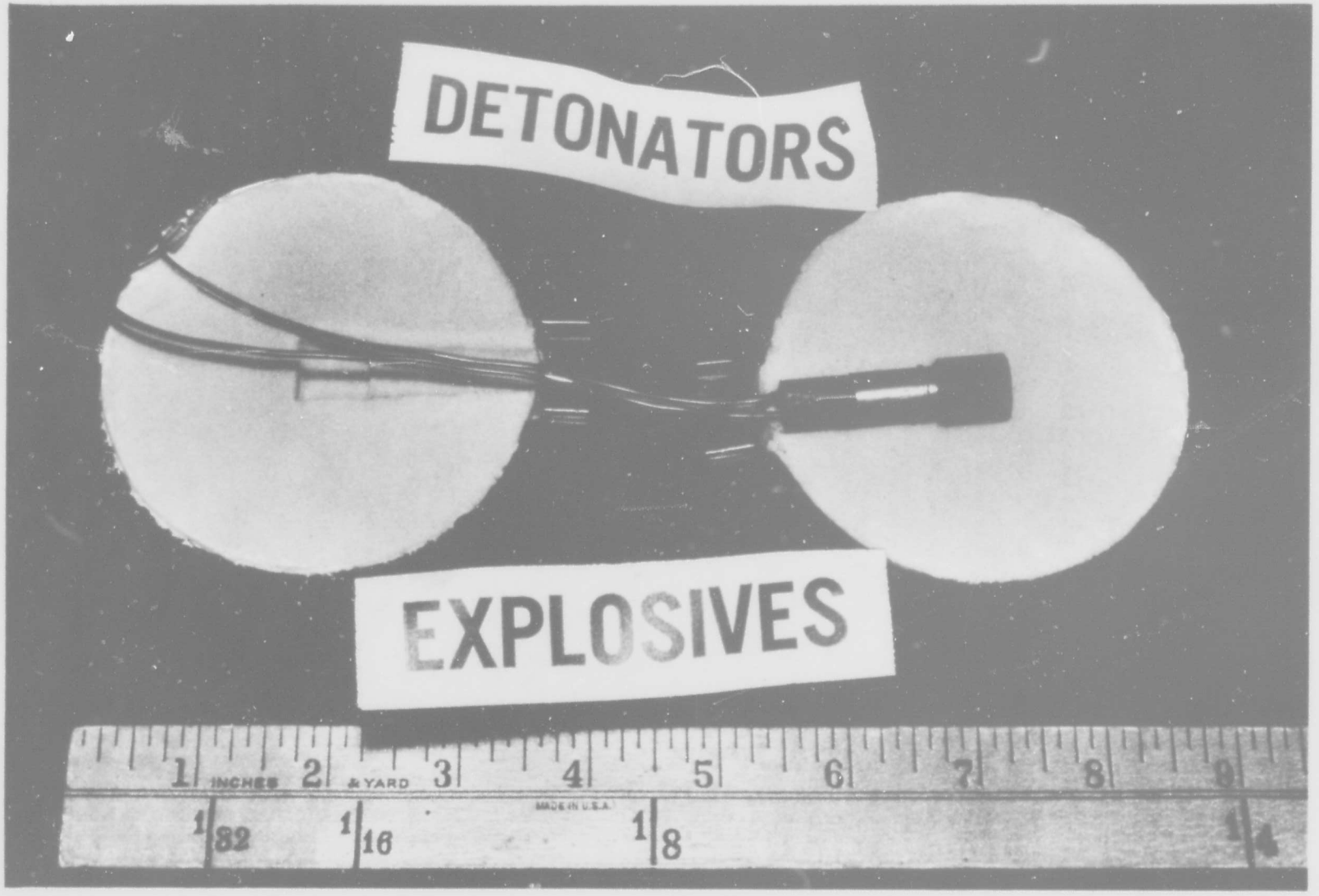

Figure 2.3 Spherical C-4 Charge

bayonet connectors at one end and pigtail connectors at the other. The high-speed camera used for surface-motion photography was interlocked to the CDU to insure that the camera was up to speed when the detonation occurred. The photographic setup included the camera, a mixer box, a voltage regulator and a timing-light generator. The mixer box connected the camera setup to the CDU, the voltage regulator maintained the voltage which adjusted the camera speed and the timing-light generator produced a pulse-type current which activated a neon light inside the camera. The light imprinted a spot on the edge of the film for the purpose of computing the exact camera speed. The timing-light generator used on ZULU II could be set for 10, 100, or 1000 pulses per second.

The sequence of events for firing was as follows:

1. The camera and associated equipment were connected, aimed and focused during the shot-placement procedure.

2. The CDU was charged and the firing system was dry run. The shot was simulated by a flashbulb which was connected to one of the CDU points. A flashbulb was also used during each shot to indicate the actual detonation time.

3. Film was loaded in the camera and the camera-speed drive-motor voltage, the timing-light generator, and the length of lead film were adjusted prior to firing.

4. The actual firing sequence was initiated from inside a firing bunker. After the signal cables between the CDU and the firing panel were connected and the CDU was fully charged, the system was ready for firing. The camera was started and ran until it had attained full speed at which time a relay closed to discharge the CDU and detonate the shot.

2.4 TECHNICAL PROGRAMS

The technical programs conducted during this experimental series included crater measurements, surface-motion analysis, and ejecta distribution study. These programs are described in the following paragraphs.

2.4.1 Crater Measurements. Measurements of the apparent craters were obtained by standard survey techniques. Elevations were determined at six-inch intervals along two orthogonal axes. Profiles of the crater were drawn from these measurements in order to determine the apparent depth and radius as well as the lip crest radius, lip height, and radius of continuous ejecta.

In addition to the surface surveys, a probing rod was also pushed through the ejecta or fallback material in order to locate the boundary of undisturbed material below. It had been previously found that the probing rod would not penetrate more than about 0.03 feet of undisturbed sand without applying considerable force. Consequently, "probe profiles" defining the boundary of undisturbed material below the apparent crater were established for each cratering detonation by this technique.

Dimensions of selected craters were also compiled from aerial stereophotographs. All ZULU II shots were photographed from the catwalk over the test facility using a Fairchild K-17 camera. The stereo-negatives for selected shots were processed by American Aerial Surveys, Inc. of Covina, California, and contour maps of the postshot ground surface were prepared with a contour interval of 0.10 foot.

2.4.2 Surface Motion Studies. The measurement of time-dependent characteristics of crater formation is requisite to an investigation of cratering phenomenology. High-speed motion picture photography was used to

document the displacement and velocity histories of the mound surface in order to study the following aspects of surface motion:

1. Characteristic features of the surface motion velocities produced by the detonation to include the velocities and times associated with peaks in motions or distinct changes in the nature of the motions.

2. Variations in these observed characteristic features with distances from surface ground zero (SGZ) and with depth of burst (DOB) of the explosion center.

3. Mound shape and size prior to venting of the cavity gas.

4. Early direction of motion as a function of preshot ground surface position.

The basic technique used to study the ground surface motion consisted of analyzing the vertical, horizontal, and total displacement histories of targets placed on the ground surface, and computing velocity histories using displacement and time increments.

Surface-motion targets were used as reference positions on the surface of the sand medium. The study of the motion of the targets is of value only if the target motion approximates the ground surface motion. The criteria for well-designed targets include the following:

1. Mass and density compatible with that of the medium.

2. Good coupling of the target into the ground.

3. High contrast markings for accurate visual analysis of target position.

The above criteria were not easily satisfied in the ZULU II sand medium. There was no difficulty in matching the average target density with the sand density; however, because target dimensions were necessarily

large (for visual analysis), the target mass was greater than that of the average clump of sand in the rising mound. Due to the fact that the sand lost its cohesion rapidly during early motion, the targets could not be adequately coupled to the medium for any extended length of time.

Two basic target designs were used in the tests. The base of one type of target was a 2-inch OD aluminum pipe which was firmly pressed into the ground. The sand which filled the pipe provided the bulk of the target mass. The other type of target, which was considered the more satisfactory of the two, had a much smaller mass than the sand-filled target and was coupled to the ground by an aluminum spike extending from the base. When emplaced in the ground, the center of gravity of this second type was at ground level.

Push-rod targets were used in an attempt to measure the motion of the subsurface. The push rods were 1/2-inch-diameter lucite rods with discs glued at the bottom. The rods were emplaced vertically in the ground with their bases at known depths and distances from the shot point. The tops of the rods extended above ground and were designed to be readily visible in the photography. The targets were placed in a line extending on either side of SGZ, perpendicular to the line of sight of the camera. The number of targets and the target positions varied for the different detonations.

The Red Lake Hy-Cam camera used in this series of experiments was capable of recording speeds of from 24 frames per second (fps) to 8000 fps. The two-speed ranges used most frequently were 700 to 1000 fps and 2500 to 3000 fps. Because of the limited film length (100 feet), the higher speed was used only when a detailed study of early motion was desired. The slower speed was used for viewing the total event, i. e. , motion from

zero time until most of the ejected sand had fallen back to the ground.

A choice of two camera lenses with focal lengths of 28mm and 55mm allowed fields of view of 12. 6 feet (horizontal) by 9. 0 feet (vertical), for study of overall mound motion, and 6. 4 feet (horizontal) by 4. 6 feet (vertical) for more detailed photography of SGZ and the push rods near SGZ.

White plywood panels were used in the background to provide contrast for targets and the growing mound. Crosses of black tape were placed on the panels to serve as stationary reference points for the surface motion targets.

A Press 22 flashbulb was used to indicate the time of detonation. Although the rise time to peak intensity was about 25 msec, tests showed that the flashbulb was activated at the same time as the bridge wire detonators in the charges.

Three film types, Double X negative black and white, Tri X negative black and white, and High-Speed Ektachrome (HSE) color, were used in the course of these experiments. The Double X negative film provided the high-contrast photography for the widest range of lighting conditions. The more grainy Tri X negative was used during poor lighting conditions, particularly at higher camera recording speeds. The HSE film required good lighting. Lighting was provided by natural daylight through the shelter roof which was opened prior to shot time. Shadows from roof beams sometimes obscured the targets.

A digitizing microscope was used for analyzing surface motion films. In this technique, the film is placed on a platform under a microscope and the platform is moved manually be means of vernier screws until a target is positioned under the cross hairs. By depressing a foot pedal,

the film position coordinates are automatically punched on an IBM card which is used as the input into the displacement and velocity calculation computer code. The computer code calculates the vertical and horizontal (x and y) displacements of targets at specific times and prints this information in tabular form. The code also calculates x and y velocities ($\dot{x}$ and $\dot{y}$) by measuring the change in displacement for finite time intervals. For example, if $y\ (t_n)$ represents the vertical displacement of a given target at time t_n (n is the number of the picture frame), then the vertical velocity is approximated by:

$$\dot{y}\ (t_{n+1/2}) = \frac{y\ (t_{n+1}) - y\ (t_n)}{t_{n+1} - t_n} = \frac{\Delta y\ (t_n)}{\Delta t_n}$$

in which $t_{n+1/2} = 1/2\ (t_{n+1} + t_n)$

The velocities, x and $\dot{y}$, are printed in tabular form. Velocity-time profiles were drawn using this information. The profiles were used to show the velocity histories of the targets.

2.4.3 Ejecta Studies Project ZULU II provided an opportunity to study in detail the origin of the fallback material which comprises the walls of the apparent crater and the ejecta forming the lip. It was necessary to mark the original position of the material in such a manner that final displacements could be measured. This was accomplished by the placement of different colored sand layers horizontally within the material to be cratered, and also by the use of numbered ejecta "pellets" placed at known locations within the material.

Since the pit was backfilled prior to each shot, small batches of sand were colored with a concrete coloring compound and placed in forms to provide blocks of colored sand 6-inches thick. These blocks were

emplaced in a 'staircase' arrangement as shown in Figure 2. 4. After the shot was fired, a trench was excavated to expose the disturbed sand layers which were photographed through a 6-inch wire grid to record the displacement of the various colored layers.

The ejecta pellets consisted of 1-inch-diameter spheres which were made of stainless steel, brass, or teflon. The spheres were placed in a vertical plane extending out from the Zero Point and their positions and identifying numbers were recorded. After the shot, the spheres were carefully uncovered and their elevation and horizontal displacement were noted. A level was used to determine the elevation of the pellets and the horizontal positions were determined using a transit and tape. These data were reduced by computer to give the elevation and horizontal coordinates from the shot point.

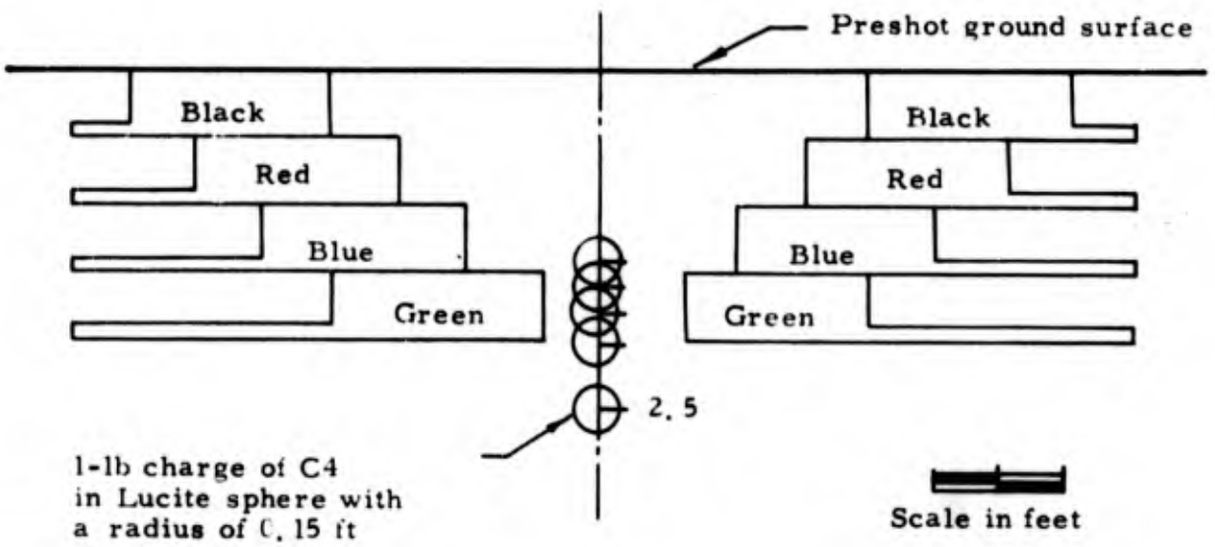

Preshot Colored Sand
Layer Arrangement

Figure 2.4

CHAPTER 3

EXPERIMENTAL RESULTS

This chapter presents experimental results used in the analysis of crater measurements, surface motion studies, and ejecta and displacement phenomena.

3.1 CRATER MEASUREMENTS

The relationship between the depth of burst, (DOB) and the apparent radius and depth of the crater obtained by conventional survey techniques is shown in Figure 3.1. It is evident that the largest craters are formed at a DOB of approximately 1.5 feet and that no apparent crater is formed at a DOB greater than about 2.1 feet.

Measurements of selected craters were also made from contour maps prepared from aerial stereophotographs. The dimensions obtained by this technique, described by Spruill and Paul[6], are also shown in Figure 3.1. Although all craters were photographed with the aerial camera, topographic maps were only prepared for a representative few. Crater dimensions determined from the maps represent a true average for the entire crater compared to the dimensions obtained from a few surface profiles.

Representative crater cross sections for the full range of DOB's in this series are illustrated in Figure 3.2A - 3.2D. The cross sections were obtained from surface surveys and show the original ground surface, the resulting crater surface, and a dashed line which is the probe profile on the boundary of the undisturbed medium. A representative series of topographic contour maps for the full range of DOBs are shown in Figures 3.3A to 3.3F and a tabular summary of crater measurements is given in Table 3.1.

Cratering Curves for One-Pound ZULU II Single-Charge Craters

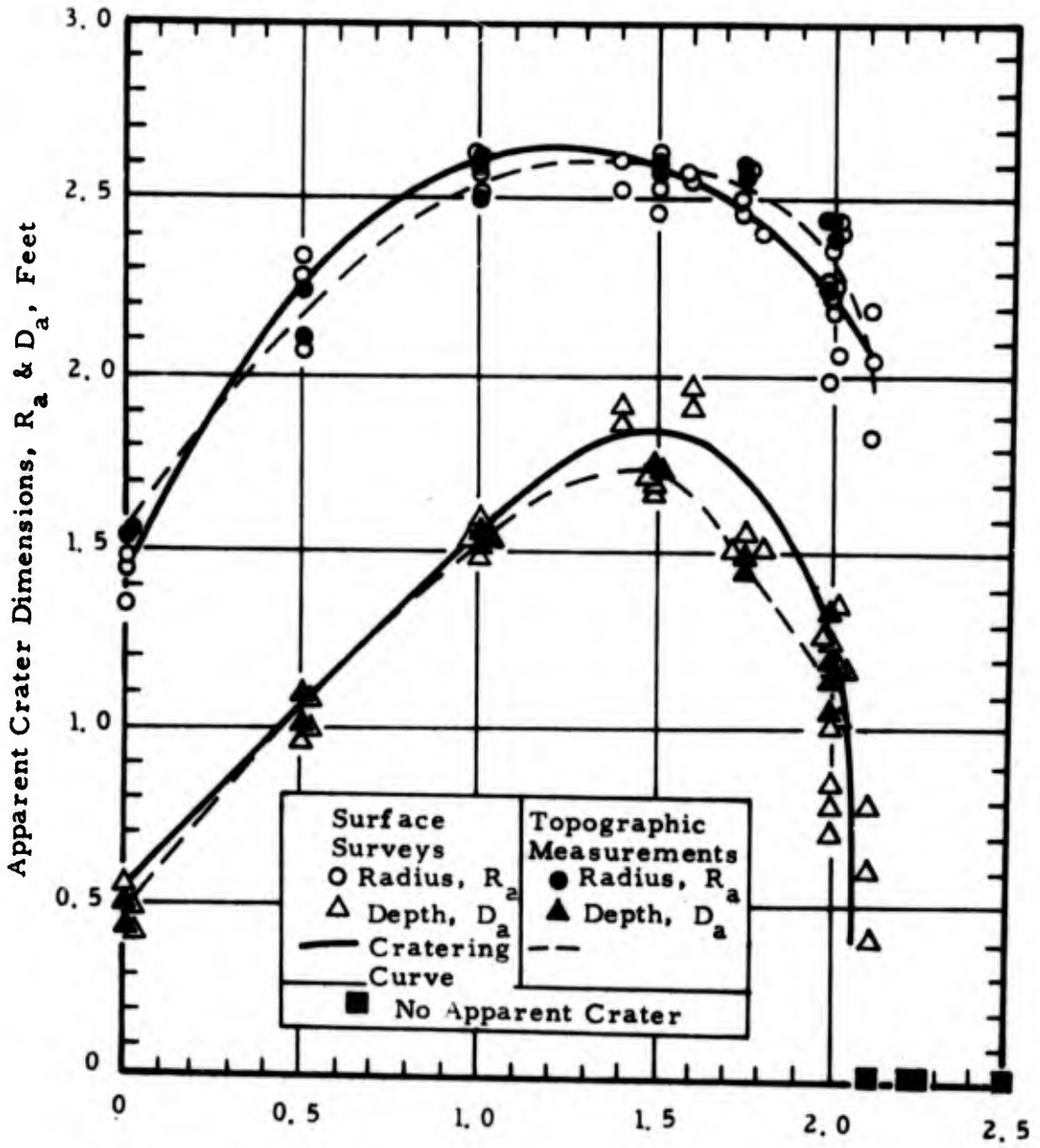

Figure 3.1

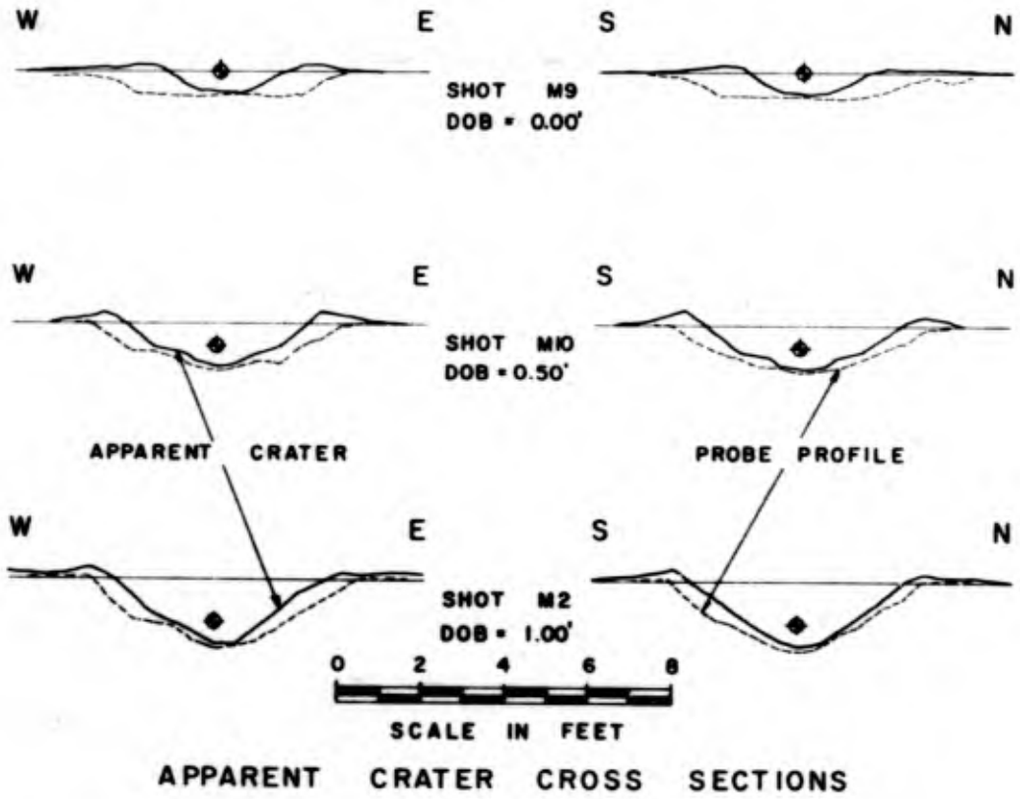
W
E
S
N
SHOT M9
DOB = 0.00'
W
E
S
N
SHOT M10
DOB = 0.50'
APPARENT CRATER
PROBE PROFILE
W
E
S
N
SHOT M2
DOB = 1.00'
0 2 4 6 8
SCALE IN FEET
APPARENT CRATER CROSS SECTIONS

Figure 3.2A

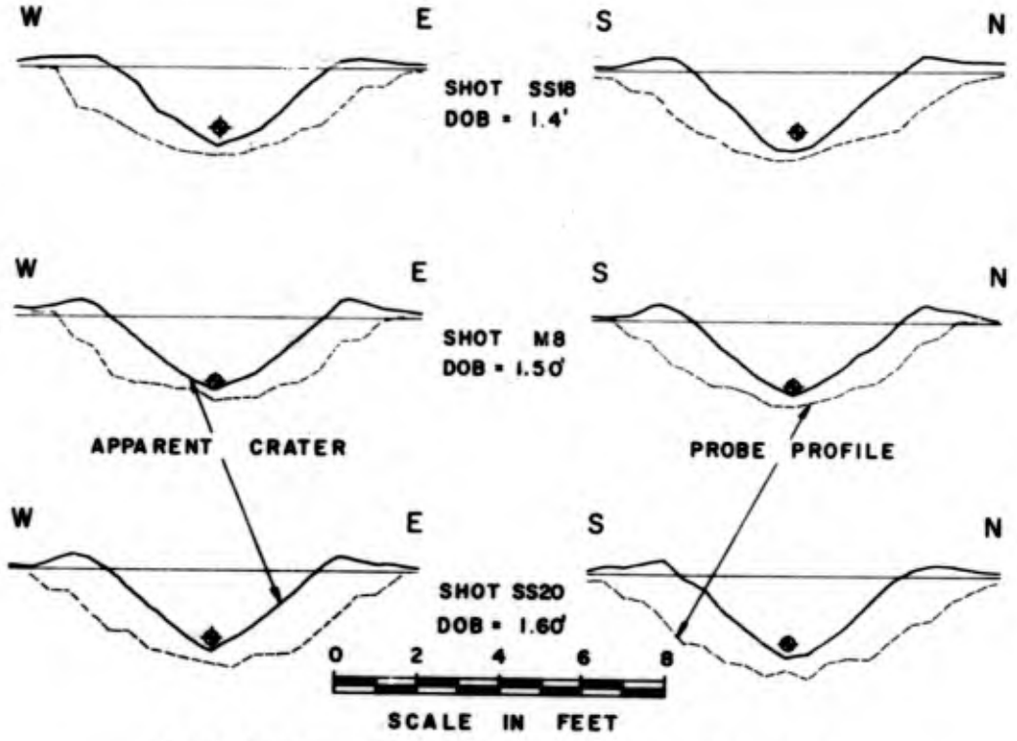

APPARENT CRATER CROSS SECTIONS

Figure 3.2B

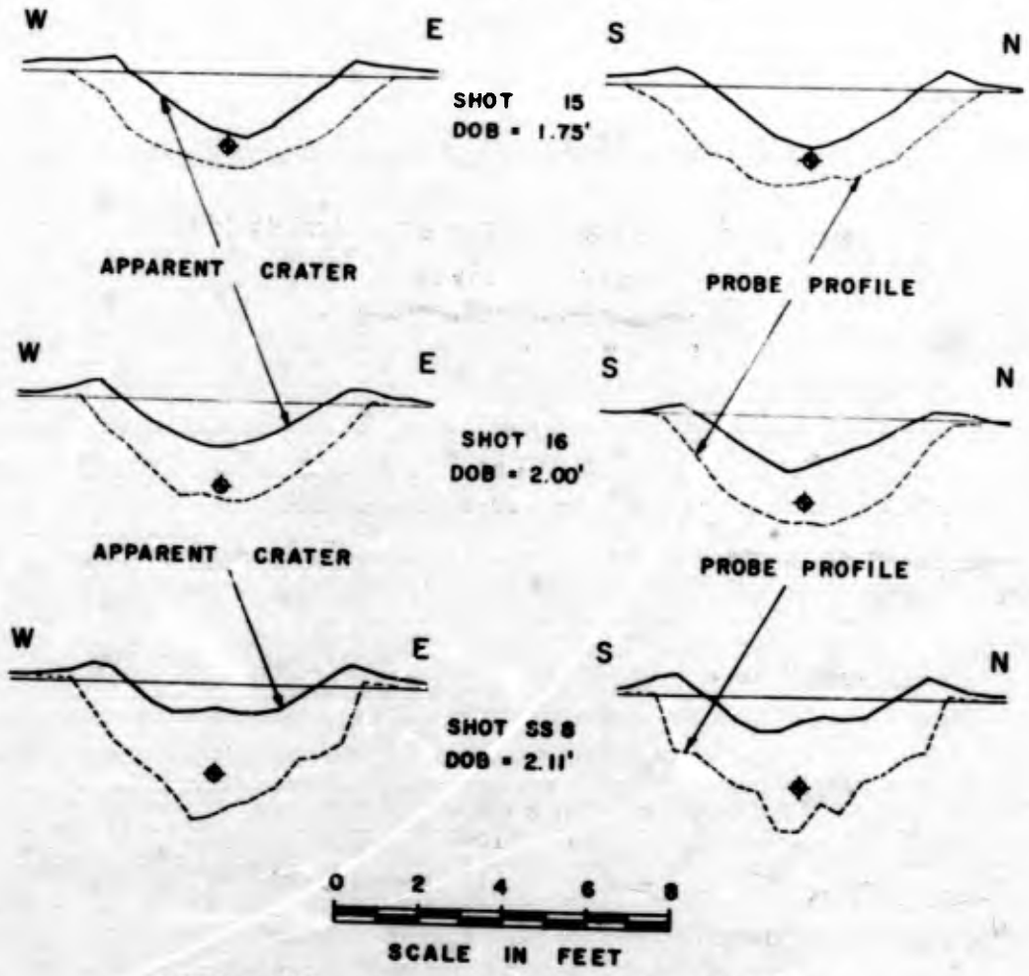

APPARENT CRATER CROSS SECTIONS

Figure 3.2C

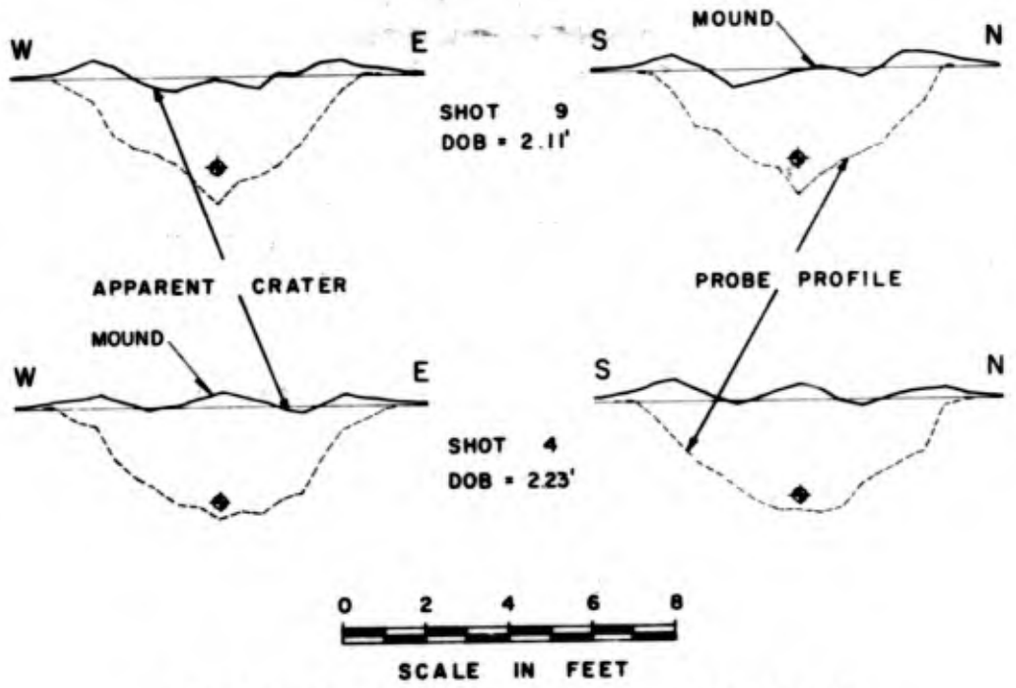

APPARENT CRATER CROSS SECTIONS

Figure 3. 2D

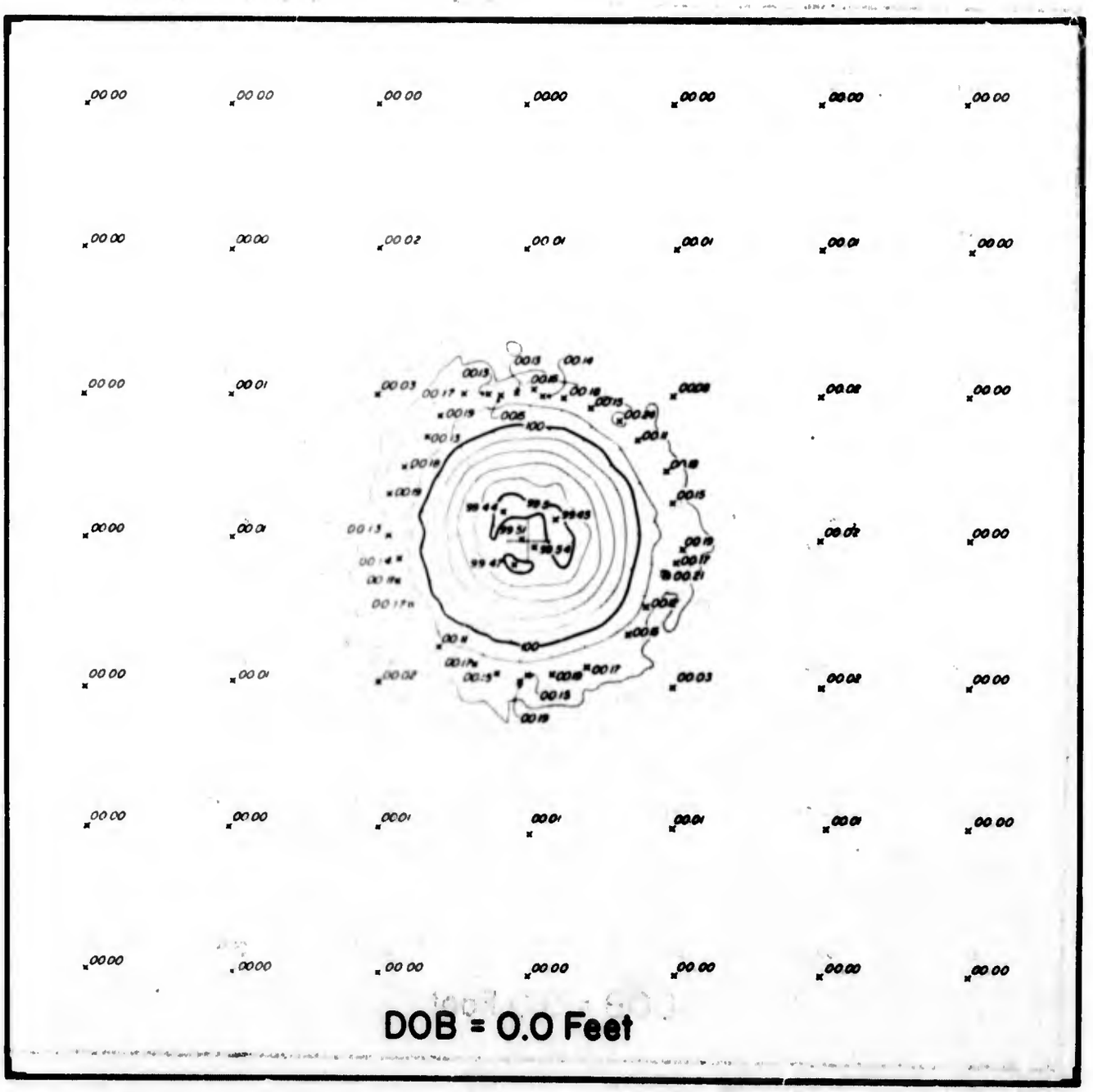

PROJECT ZULU II-SHOT M9

POST SHOT TOPOGRAPHY

SCALE

1 0.5 0 1 2 3 4 5

FEET

Figure 3.3A

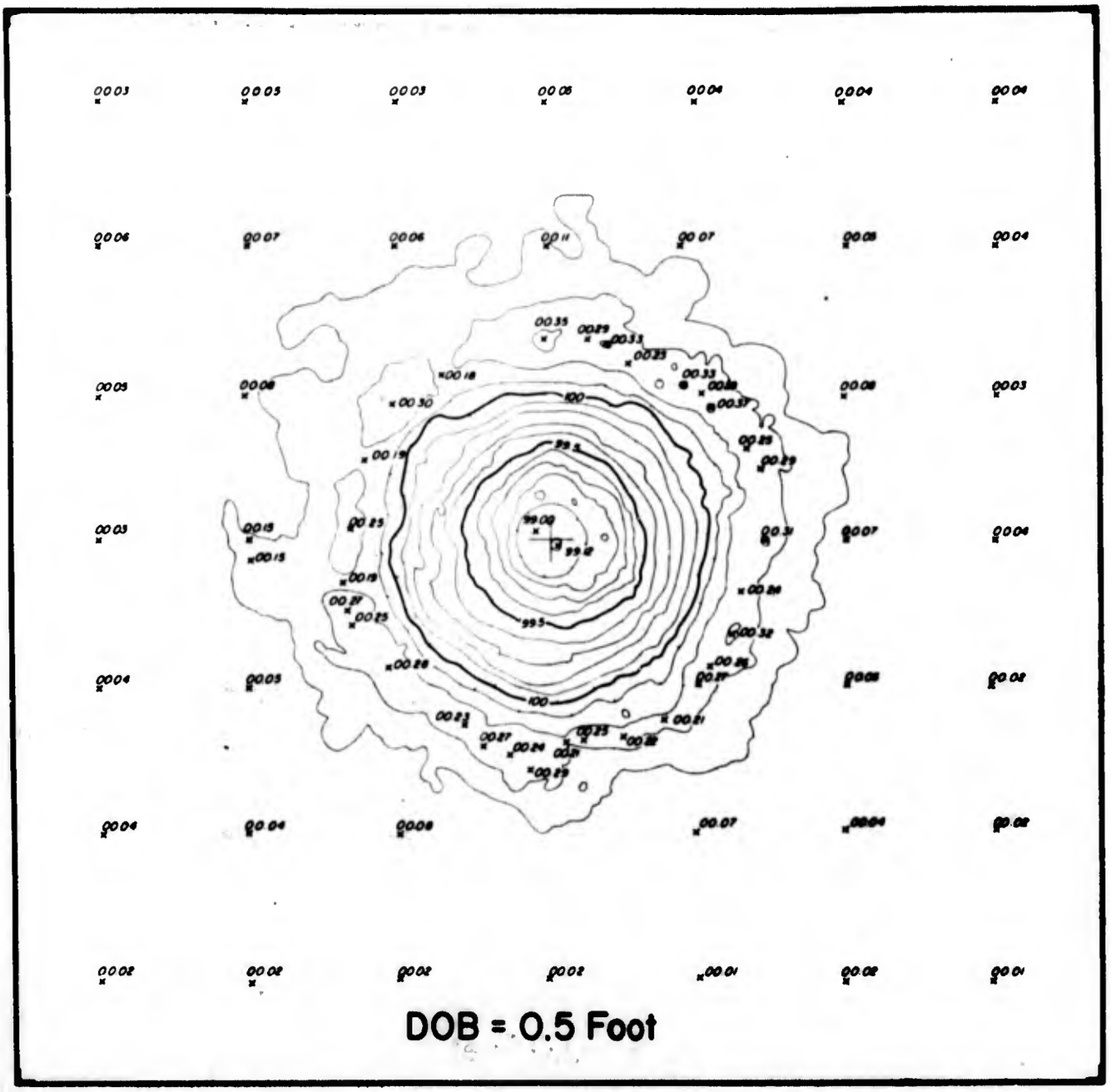

PROJECT ZULU II-SHOT M7

POST SHOT TOPOGRAPHY

SCALE

1 0.5 0 1 2 3 4 5

FEET

Figure 3.3B

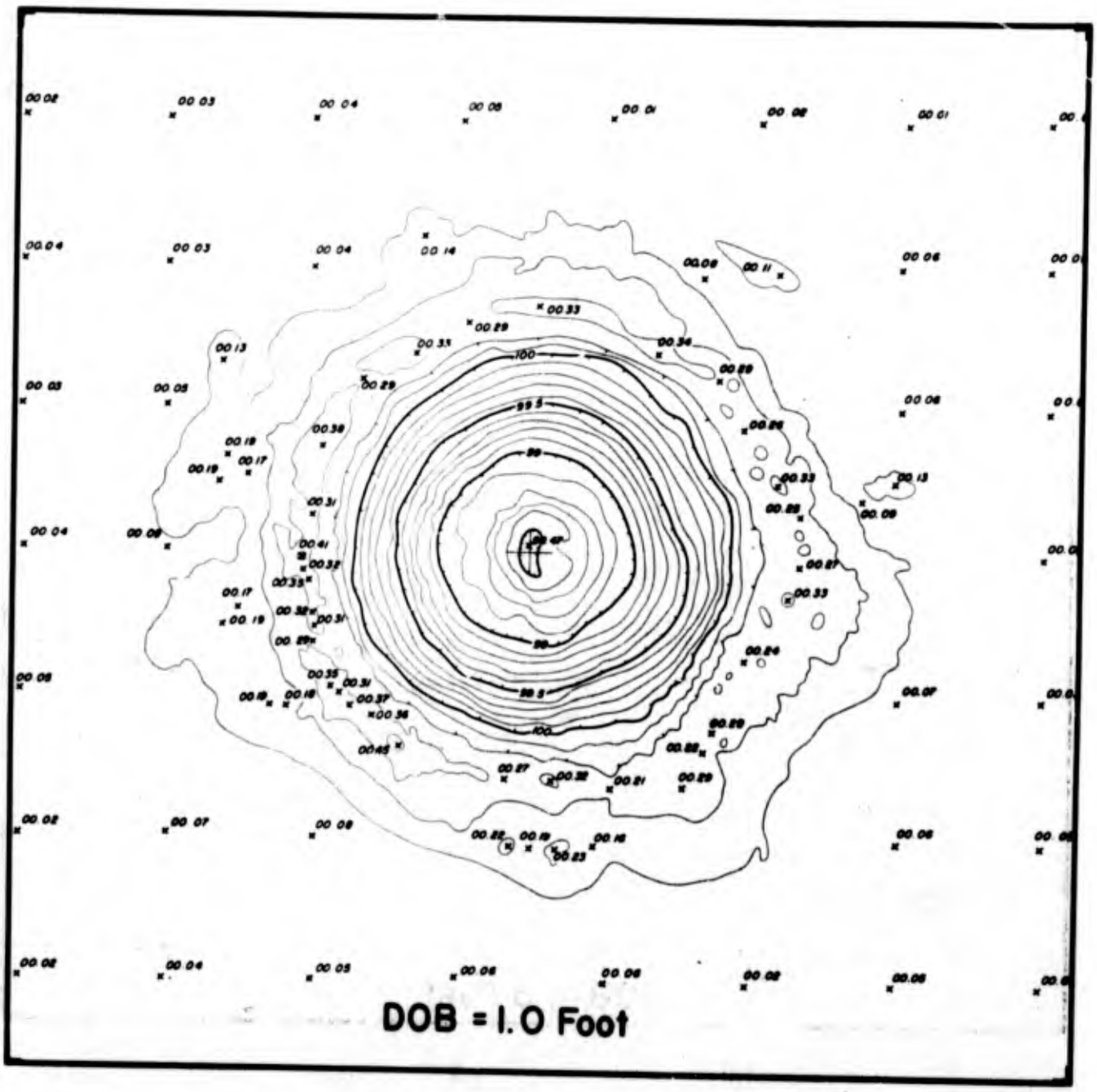

PROJECT ZULU II-SHOT M4

POST SHOT TOPOGRAPHY

SCALE

1 0.5 0 1 2 3 4 5

FEET

Figure 3. 3C

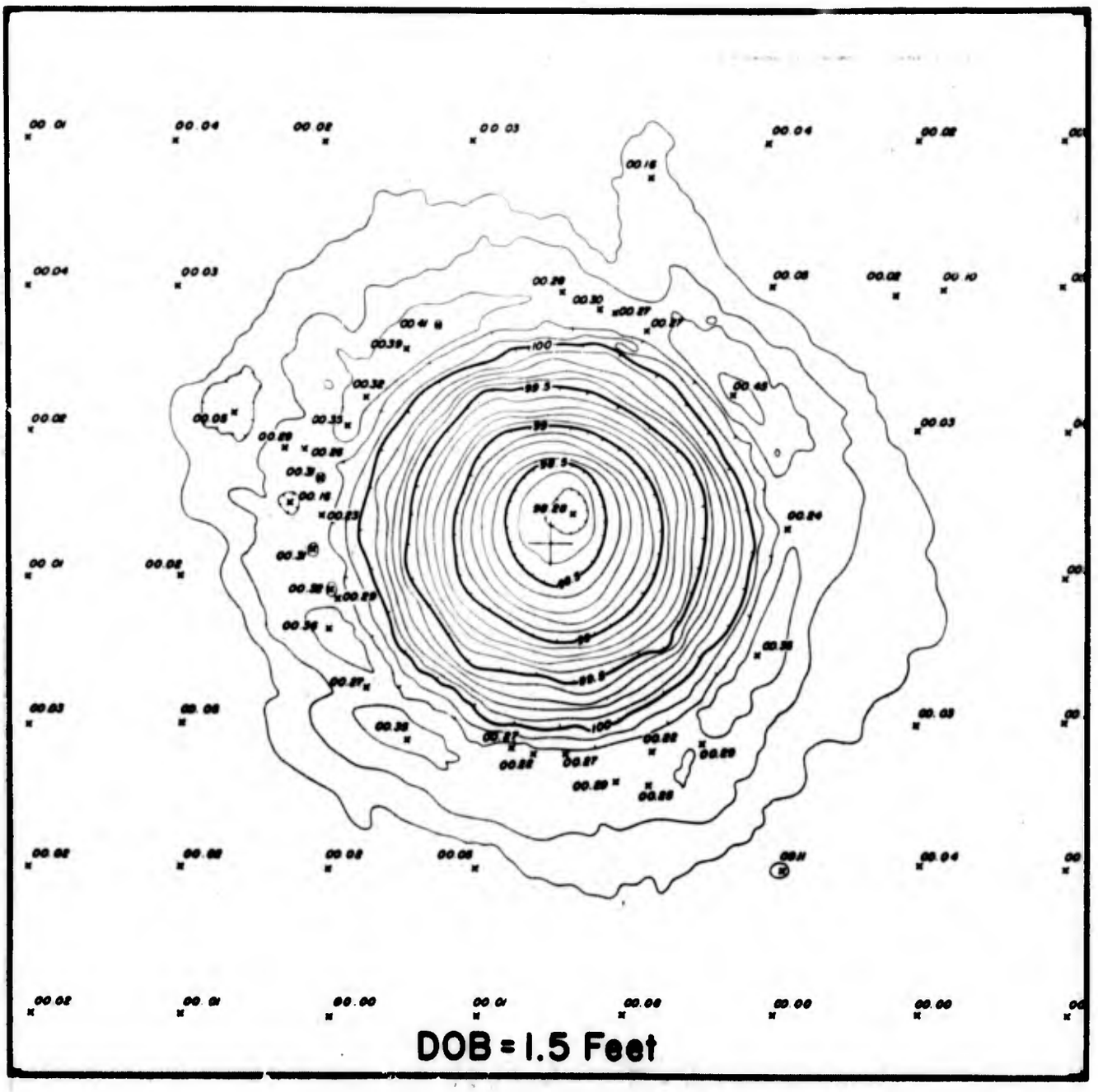

PROJECT ZULU II-SHOT M1

POST SHOT TOPOGRAPHY

SCALE

1 0.5 0 1 2 3 4 5

FEET

Figure 3.3D

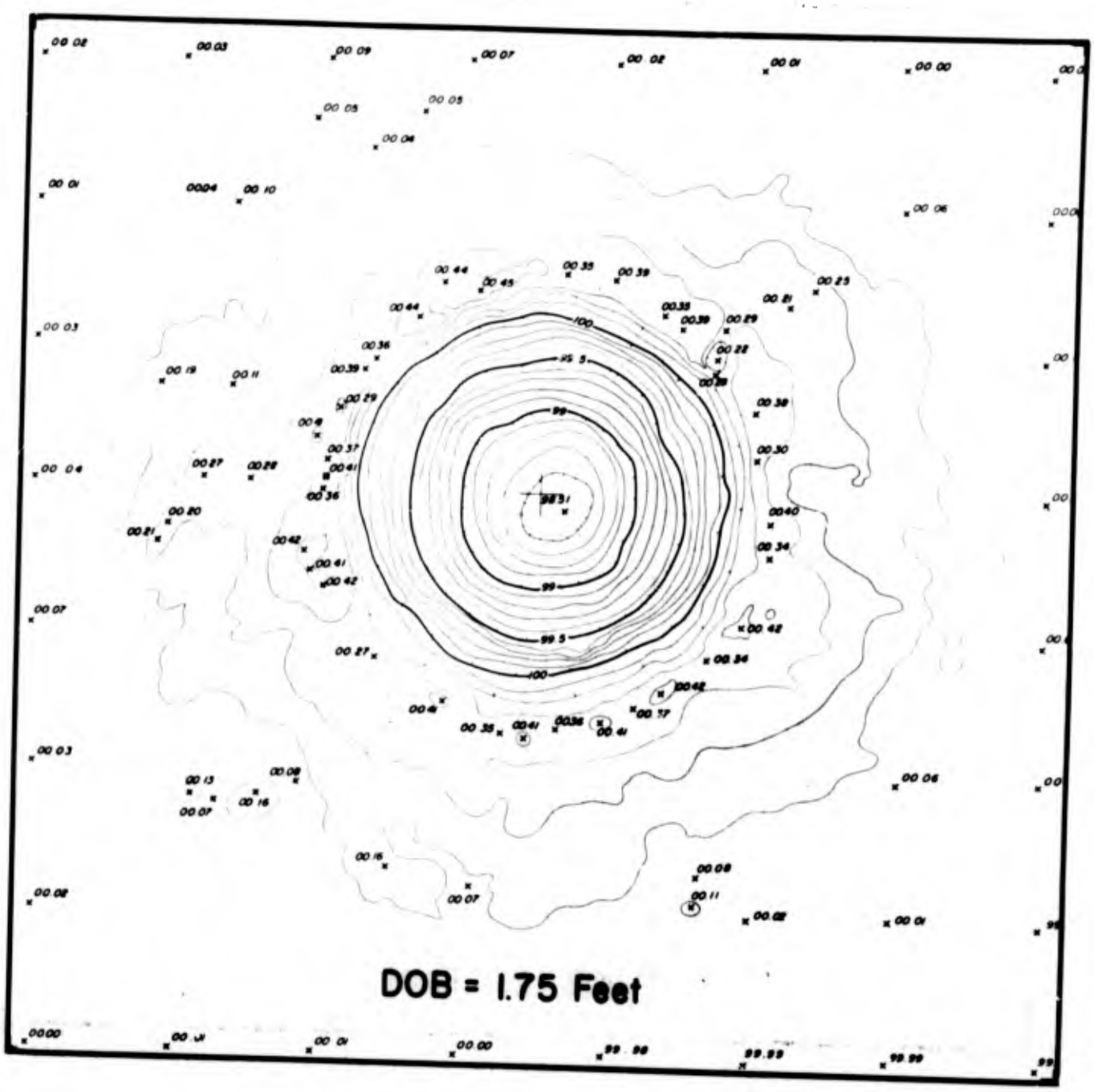

PROJECT ZULU II-SHOT 15 PORT C

POST SHOT TOPOGRAPHY

SCALE

1 0.5 0 1 2 3 4 5

FEET

Figure 3.3E

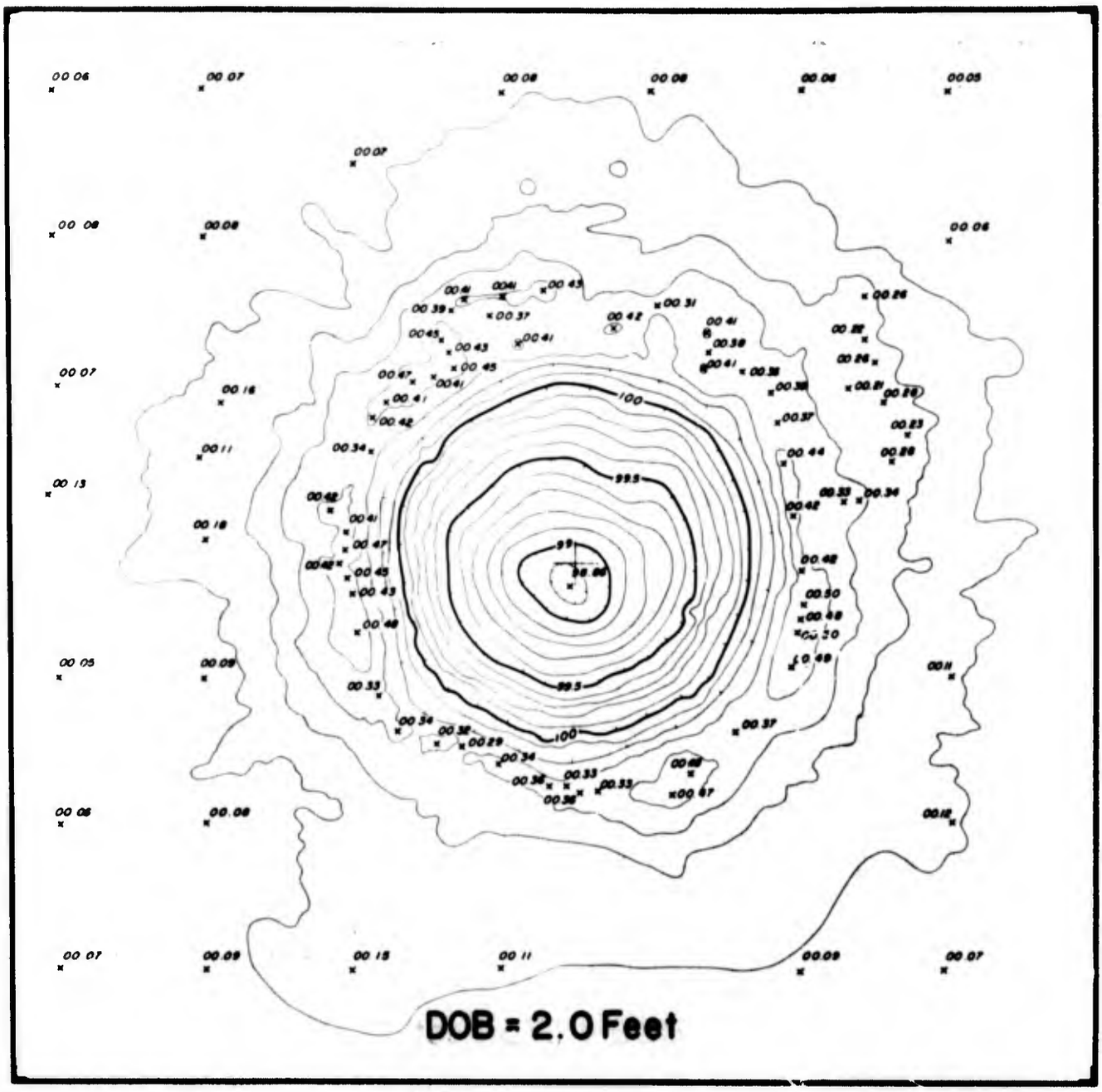

PROJECT ZULU II-SHOT 16

POST SHOT TOPOGRAPHY

SCALE

1 0.5 0 1 2 3 4 5

FEET

Figure 3. 3F

TABLE 3.1

SUMMARY OF RESULTS FOR SINGLE-CHARGE CRATERS

All charges were one-pound C-4 spheres center-detonated

DOB	Shot No.	D_a	R_a	H_{al}	R_{al}	R_{eb}	D_p	R_p	V_{max}	Dry Density	Postshot Density
feet		feet	feet	feet	feet	feet	feet	feet	fps	pcf	pcf
0	M9	0.52	1.48	0.125	2.00	5.00	0.65	4.00	3200	111.2	90.9
0	M11	0.53	1.34	0.163	1.85	5.00	0.55	3.00	ND	110.6	ND
0	M12	0.50	1.44	0.195	2.00	4.75	0.60	2.50	ND	110.6	ND
0.50	M6	1.09	2.34	0.240	2.90	8.25	1.20	4.00	ND	109.9	91.0
0.50	M7	0.98	2.07	0.254	2.83	11.50	1.15	3.62	ND	113.6	ND
0.50	M10	1.00	2.28	2.245	2.75	9.45	1.10	3.00	1240	110.6	ND
1.00	M2	1.51	2.55	0.220	3.00	9.00	1.65	3.13	ND	114.5	ND
1.00	M4	1.55	2.64	0.308	3.43	11.30	1.65	3.50	301	110.4	90.6
1.00	M5	1.60	2.54	0.283	3.13	9.60	1.75	4.00	ND	110.2	ND
1.40	SS18	1.89	2.61	0.290	3.25	14.00	2.10	4.50	174	111.8	95.2
1.40	SS19	1.92	2.53	0.315	3.40	ND	2.15	5.62	161	110.9	93.9
1.50	M1	1.74	2.63	0.264	3.25	11.20	1.90	3.13	ND	110.2	92.0
1.50	M3	1.73	2.46	0.356	3.53	10.80	2.05	4.00	100	109.8	ND
1.50	M8	1.76	2.54	0.398	3.20	14.00	2.00	4.13	ND	110.7	87.5
1.60	SS17	1.97	2.57	0.380	3.38	12.00	2.33	4.63	110	111.8	96.2
1.60	SS20	1.91	2.55	0.363	3.25	ND	2.41	4.63	90	111.8	94.4
1.75	15	1.55	2.50	0.394	3.08	9.75	2.40	4.13	80	114.3	ND
1.75	8	1.49	2.47	0.301	3.12	9.00	2.50	3.88	70	114.1	ND
1.80	SS21	1.51	2.41	0.390	3.00	ND	2.52	4.63	84	111.2	ND
1.98	10	1.26	2.27	0.455	3.10	7.50	ND	ND	57	112.5	ND
1.99	SS7	0.70	1.99	0.361	2.85	6.63	3.02	3.75	44	113.6	ND

TABLE 3. 1, continued

DOB	Shot	D_a	R_a	H_{al}	R_{al}	R_{eb}	D_p	R_p	V_{max}	Dry Density	Postshot Density
feet		feet	feet	feet	feet	feet	feet	feet	fps	pcf	pcf
2.00	1	1.35	2.25	0.485	3.11	6.75	ND	ND	56	112.6	ND
2.00	16	1.17	2.41	0.336	3.00	7.75	2.45	3.50	60	115.6	108.1
2.00	19	1.08	2.24	0.495	3.00	7.15	2.40	3.87	52	110.9	ND
2.00	SS5	1.01	2.18	0.521	2.90	8.75	2.02	4.00	50	109.7	ND
2.00	SS10	1.21	2.38	0.326	3.13	8.63	2.40	4.00	53	111.9	ND
2.00	SS14	0.85	2.26	0.485	3.25	6.00	2.85	3.88	44	111.6	ND
2.00	SS16	1.02	2.44	0.385	3.25	6.00	2.83	4.50	ND	111.6	ND
2.01	SS22	0.78	2.07	0.410	3.00	ND	2.72	4.38	56	111.5	ND
2.11	SS8	0.78	2.19	0.493	3.05	ND	3.23	3.50	44	110.6	ND
2.11	SS9	0.60	1.83	0.426	2.90	7.45	2.56	3.75	45	111.9	ND
2.11	SS24	0.40	2.05	0.410	3.00	ND	2.76	4.75	42	111.4	ND
2.11	2	M	N/A	0.451	2.98	6.25	ND	ND	40	110.9	ND
2.11	9	M	N/A	0.390	2.98	7.25	3.00	3.75	39	111.0	98.4
2.23	4	M	N/A	0.310	2.98	7.50	2.70	4.13	34	112.6	ND
2.24	11	M	N/A	0.311	3.10	6.45	2.60	3.88	40	114.4	ND
2.27	3	M	N/A	0.300	3.11	9.50	ND	ND	34	112.1	ND
2.25	SS23	M	2.26	0.370	3.06	ND	3.15	4.25	ND	111.7	ND
2.50	5	M	N/A	0.361	3.33	7.40	2.90	4.25	28	112.2	ND
2.50	6	M	N/A	0.325	3.18	7.00	3.25	4.50	33	113.8	ND
2.50	SS26	M	N/A	0.410	3.00	ND	3.45	4.50	36	111.2	ND
2.76	7	M	N/A	0.354	3.10	6.75	3.50	4.38	21	114.4	ND

ND - No Data Collected.

N/A - Not Applicable (no apparent crater formed).

DOB - Depth of burst.

D_a - Apparent crater depth.

R_a - Apparent crater radius.

H_{al} - Height of apparent crater lip.

R_{al} - Radius of apparent lip crest to center.

R_{eb} - Radius of outer boundary of continuous ejecta.

D_p - Maximum depth of probe profile from original ground surface

R_p - Radius of intersection of probe profile with original ground surface.

V_{max} - Maximum velocity of SGZ target.

M - Mound formed in bottom of crater.

3.2 SURFACE MOTION STUDIES

High-speed photography provided empirical information concerning target motion during mound growth. In view of the problem of coupling the targets with the low-strength sand medium it appears that the targets performed well.

The information obtained from the surface-motion program was used to investigate the following characteristics of the mound development:

1. Time history of velocity at SGZ as a function of DOB.
2. Mound configuration at "freefall."
3. Variation of velocity with increasing distance from the SGZ.
4. Variation of maximum velocity at SGZ as a function of DOB.
5. Push Rod Motion.

Representative velocity histories for SGZ targets are shown in Figure 3.4. "Phase I" represents a rapid increase in velocity to a maximum or "freefall" velocity which is "Phase II".

Figures 3.5A through 3.5F show the "target directions and velocities at freefall" for six shots at DOB's from 1.4 to 2.24 feet. Each figure shows the mound shape at the time all targets have attained freefall. The velocities and direction of motion with respect to the vertical for each target at freefall, as well as the targets' position on the mound at that time are also shown. Theta (θ) represents the angle between the vertical and the direction of movement of the target at freefall.

The plot of early target trajectories and mound growth for shot 1 in Figure 3.6 is representative of shots at other depths of burst and illustrates the essential features of mound development. At early times the

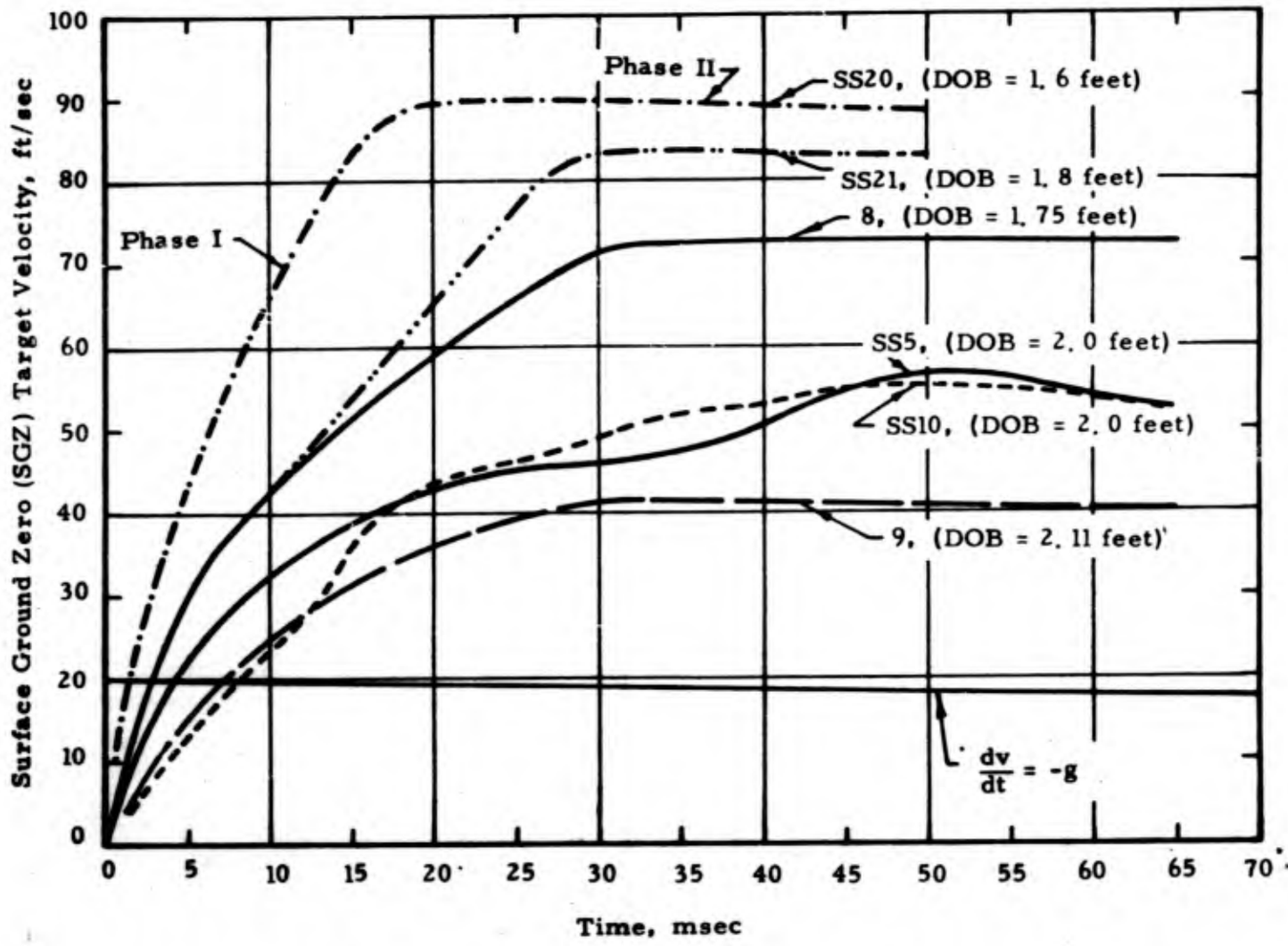

Figure 3.4 A Plot Showing Surface Ground Zero Target Velocity Compared to Time After Detonation.

SS19 DOB 1.4 feet Target Directions and Velocities at Freefall

Mound at 30 msec - All Targets in Freefall

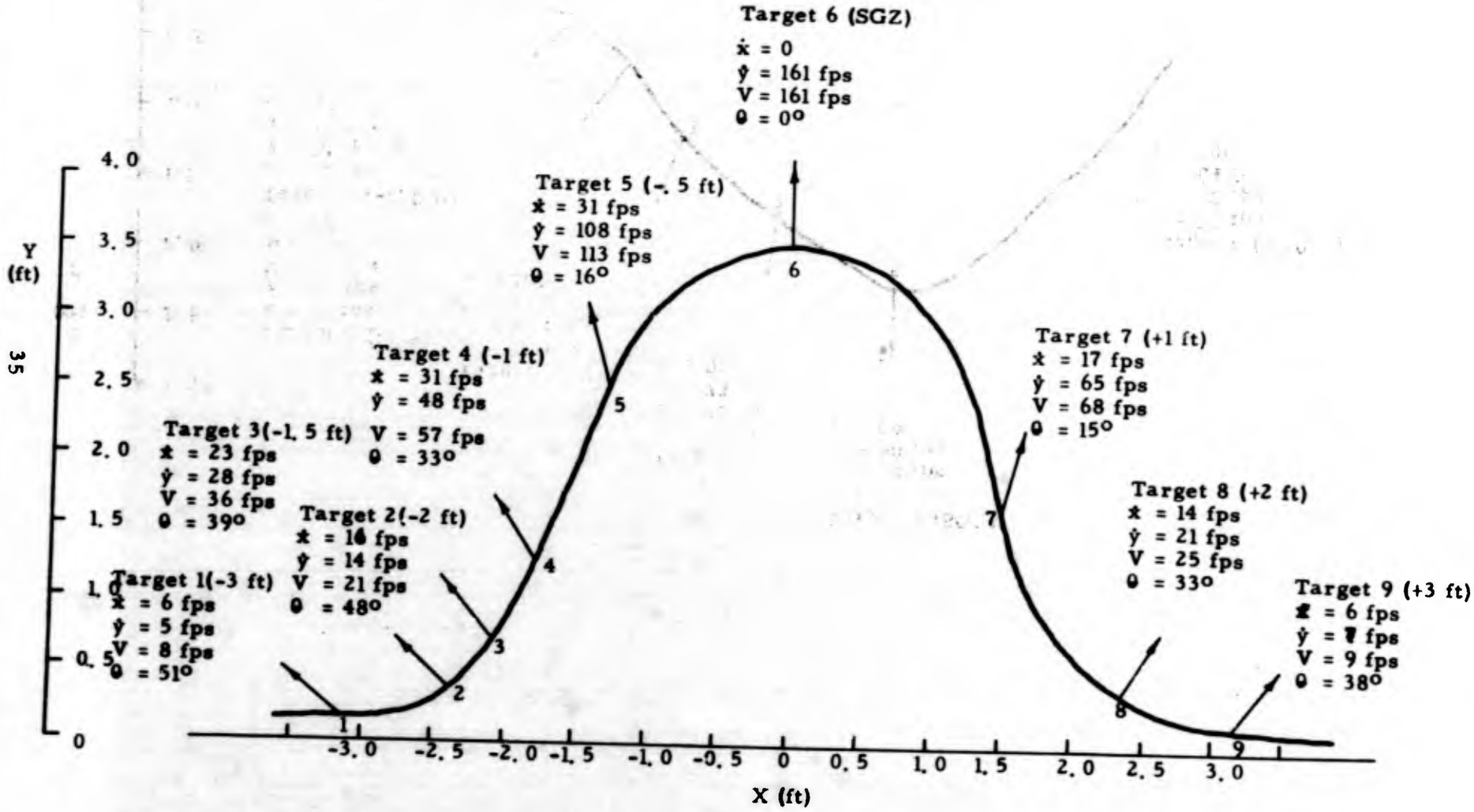

Figure 3.5A

SS20 DOB 1. 6 ft Target Directions and Velocities at Freefall

Mound at 30 msec - all targets in freefall

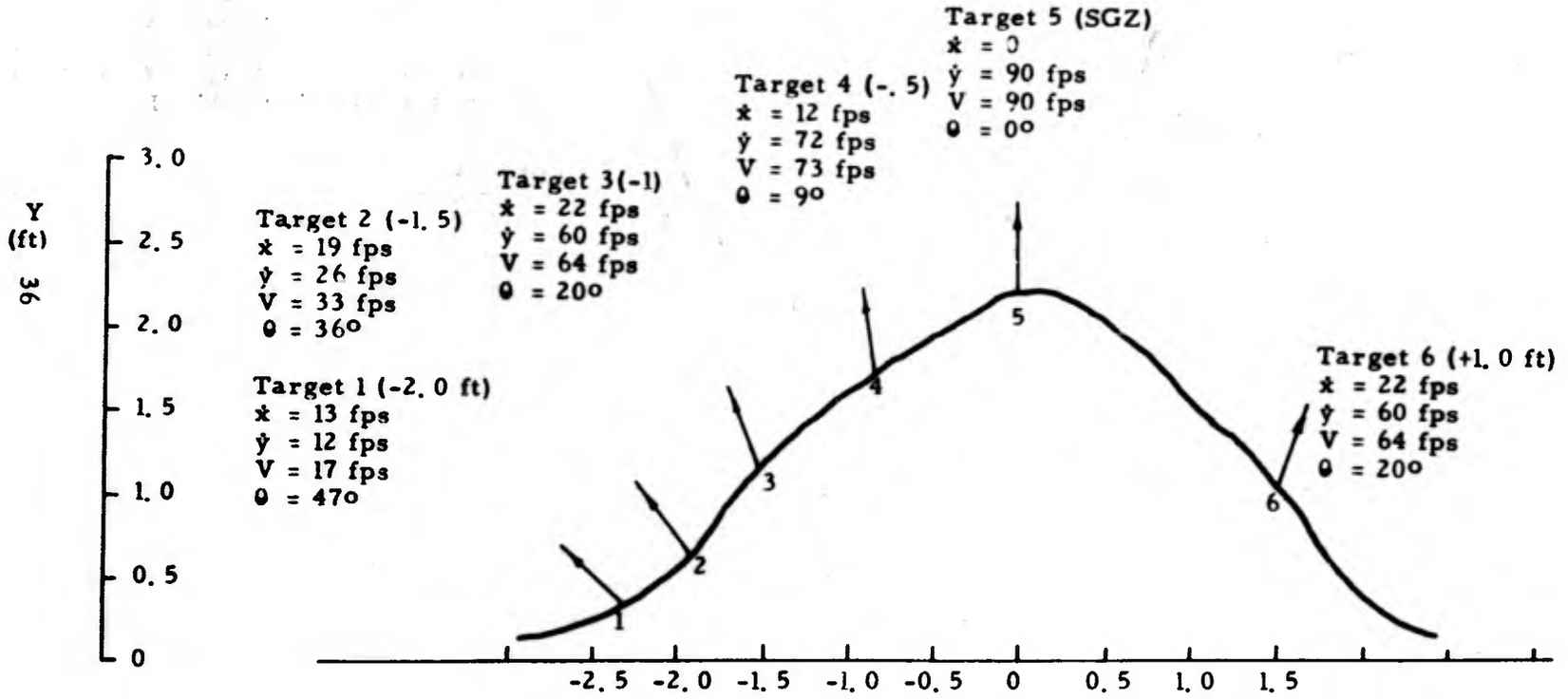

Figure 3. 5B

SS21 DOB 1. 8 ft Target Dimensions and Velocities at Freefall

Mound at 35 msec - All targets in freefall

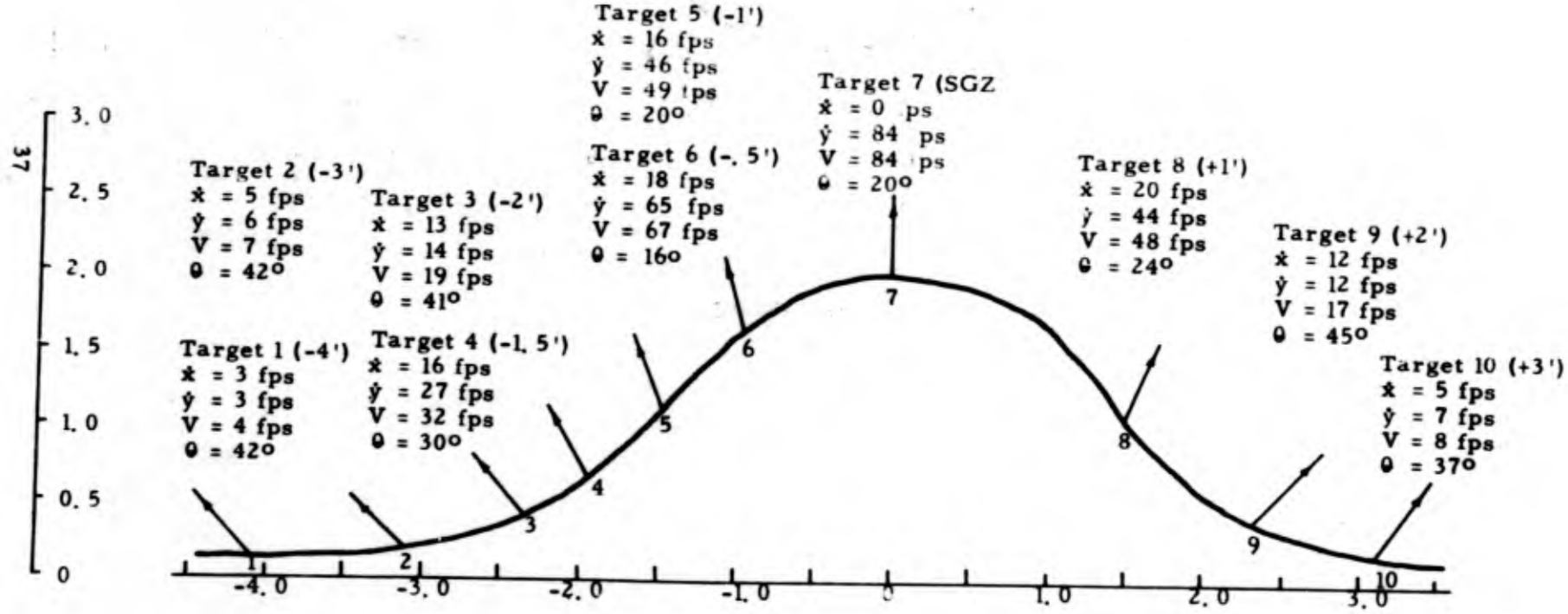

Figure 3. 5C

Shot 16 DOB 2.0 ft Target Directions and Velocities at Freefall

Mound shown at 45 msec - all targets in freefall

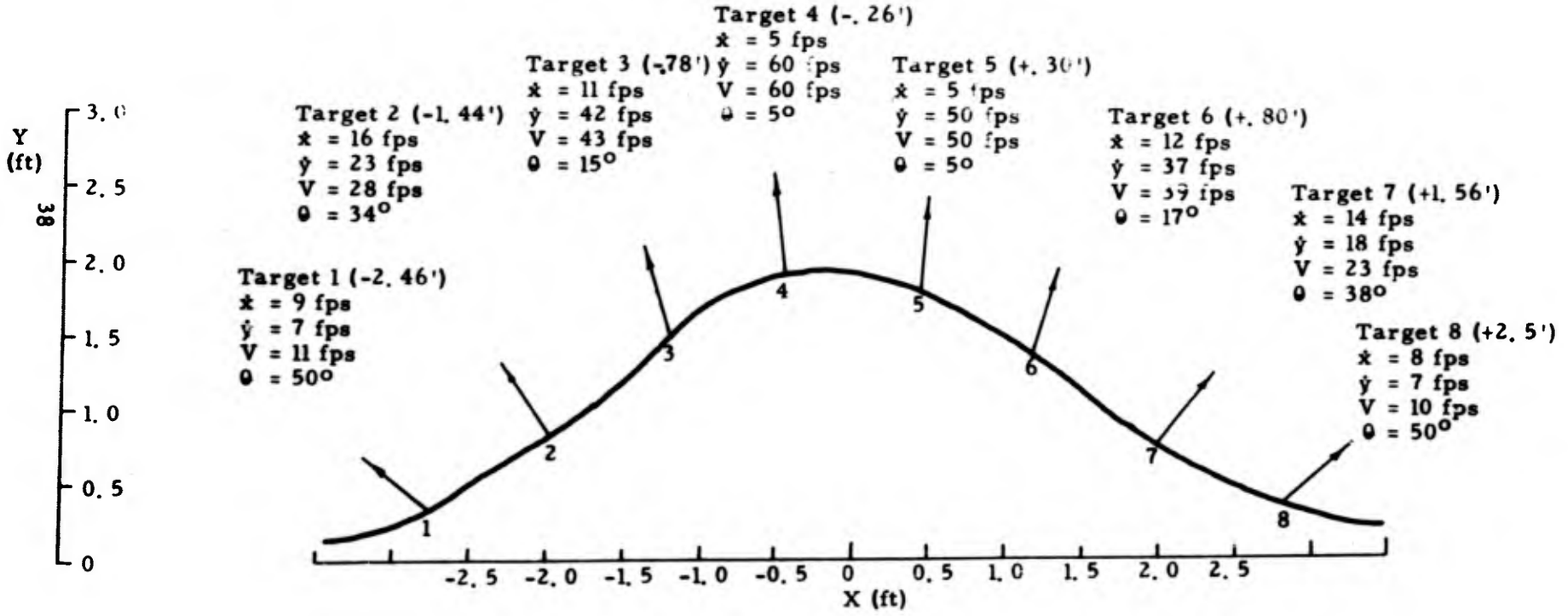

Figure 3.5D

Shot 9 DOB 2. 11 ft Target Directions and Velocities at Freefall

Mound at 45 msec - all targets in freefall

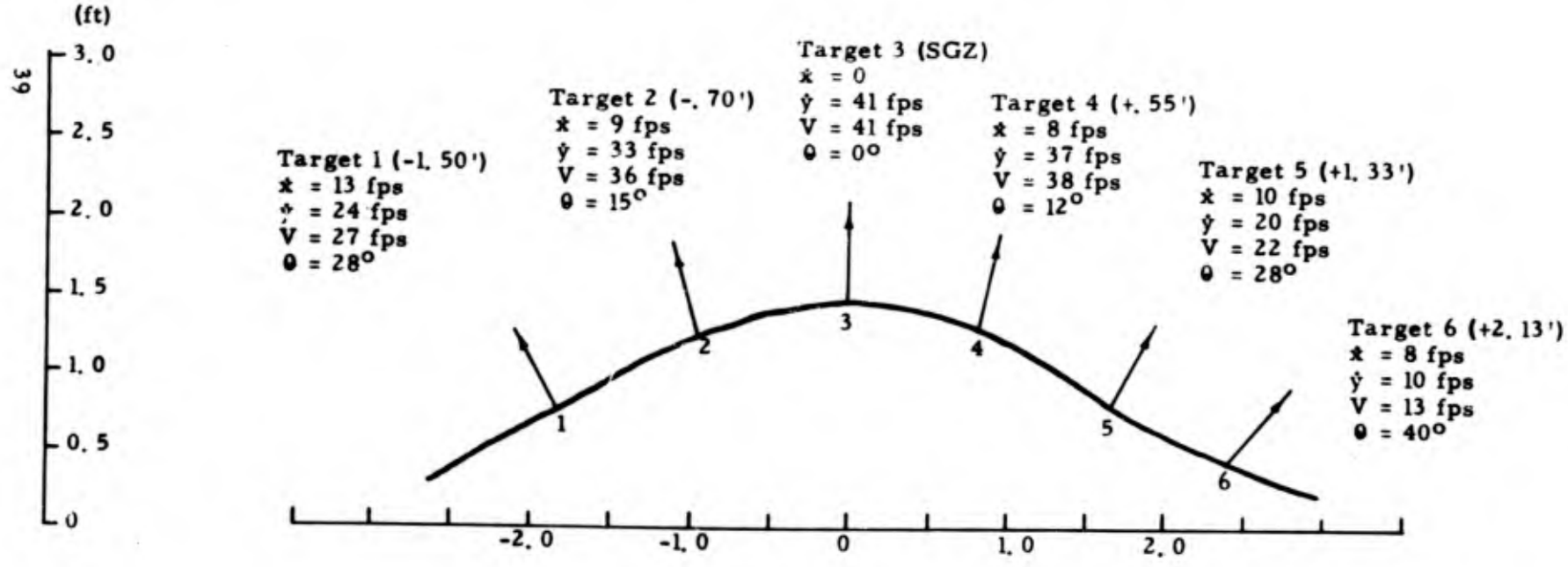

Figure 3. 5E

Shot 11 DOB 2.24 ft Target Directions and Velocities at Freefall

Mound Shown at 55 msec - All targets in freefall

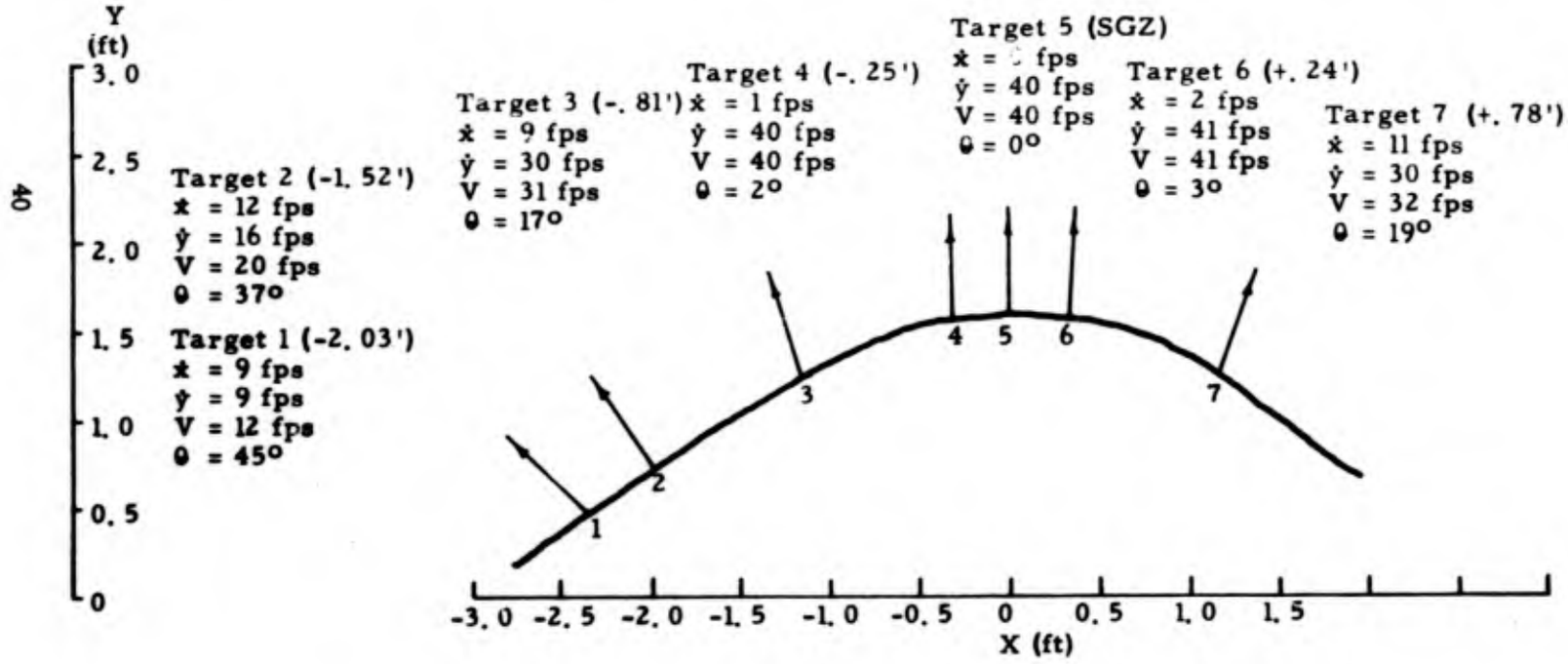

Figure 3.5F

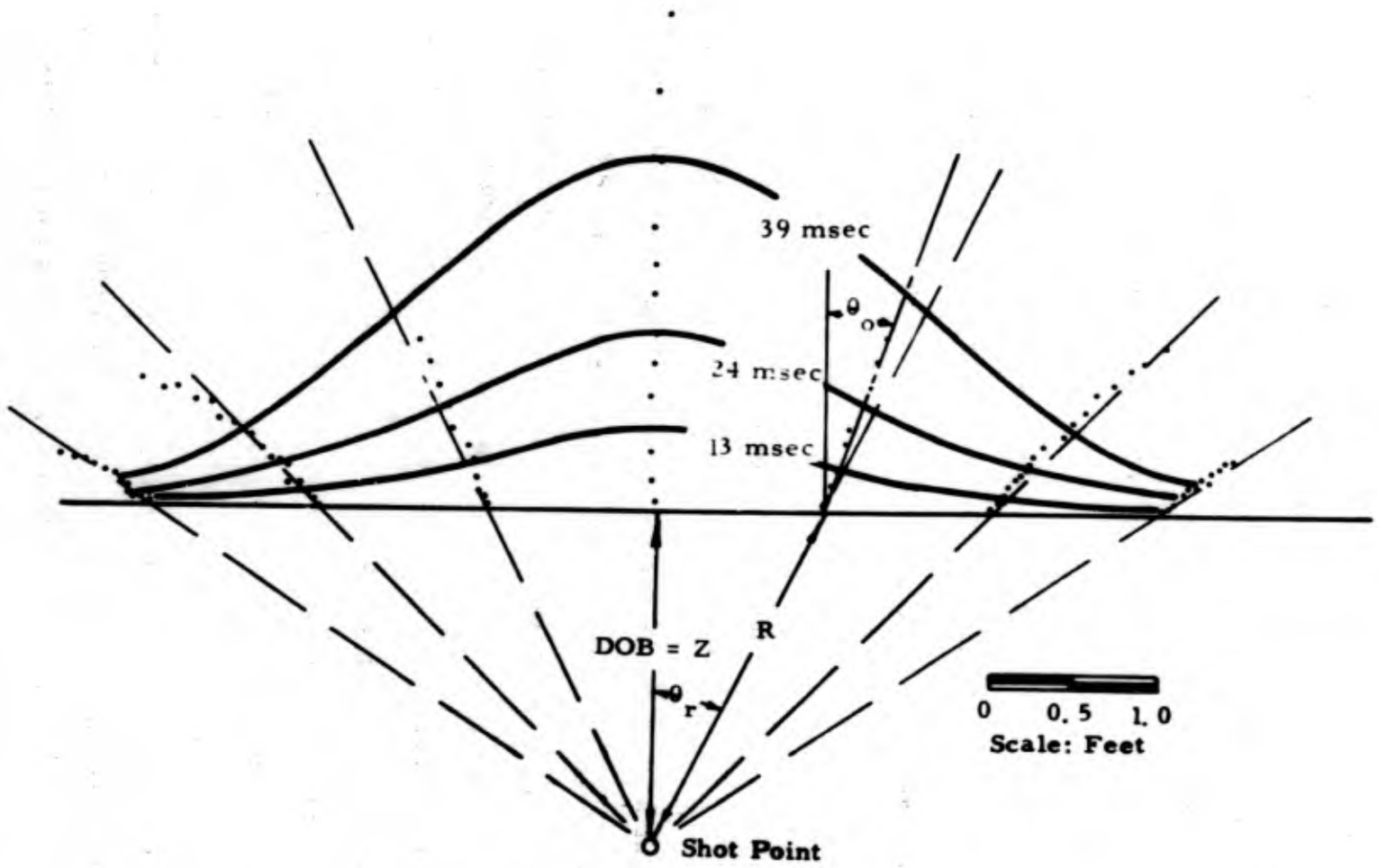

Figure 3.4 Target Trajectories and Early Mound Shape for Shot #1, (DOB = 2.0 feet)

trajectories show only a slight curvature, however, during late motion (t >70 msec) the trajectories tend toward a parabolic or ballistic free-fall path. θ_o represents the angle between the vertical and the initial direction of movement and θ_r represents the angle between the vertical and a line drawn from the preshot position of the target through the shot-point

Figure 3.7 shows a log-log plot of the maximum vertical velocity ($\dot{y}$) for each SGZ target as a function of DOB for a large number of single-charge ZULU II shots. The equation derived from the curve is:

$$\dot{y}_{max} = \frac{470}{DOB^{3.1}}$$

The push rods used for the measurement of subsurface motion were typically positioned 0.5 foot either side of ground zero with the disc bases located 0.5 foot and 1.0 foot above the shotpoint. The motion of the tops of the push rods and the angles at which the push rods slanted (in the vertical plane of the line of surface targets) were recorded. Using the known length of the push rods and the assumption that the push rods remained in the vertical plane of the line of surface targets, the motion of the push rod bases was calculated.

The motion of the push rod bases is summarized as follows:

1. The push rod bases experienced significantly higher acceleration (for a short period of time) than did the surface targets.

2. The initial motion corresponded with a shock wave travel time from the shot point to push rod base of about 1000 ft/sec.

3. The push rods initially moved with vertical velocities 5 to 10 times those experienced at the ground surface.

Peak Surface Ground Zero Velocity,
V_{max}, Compared to Depth of Burst

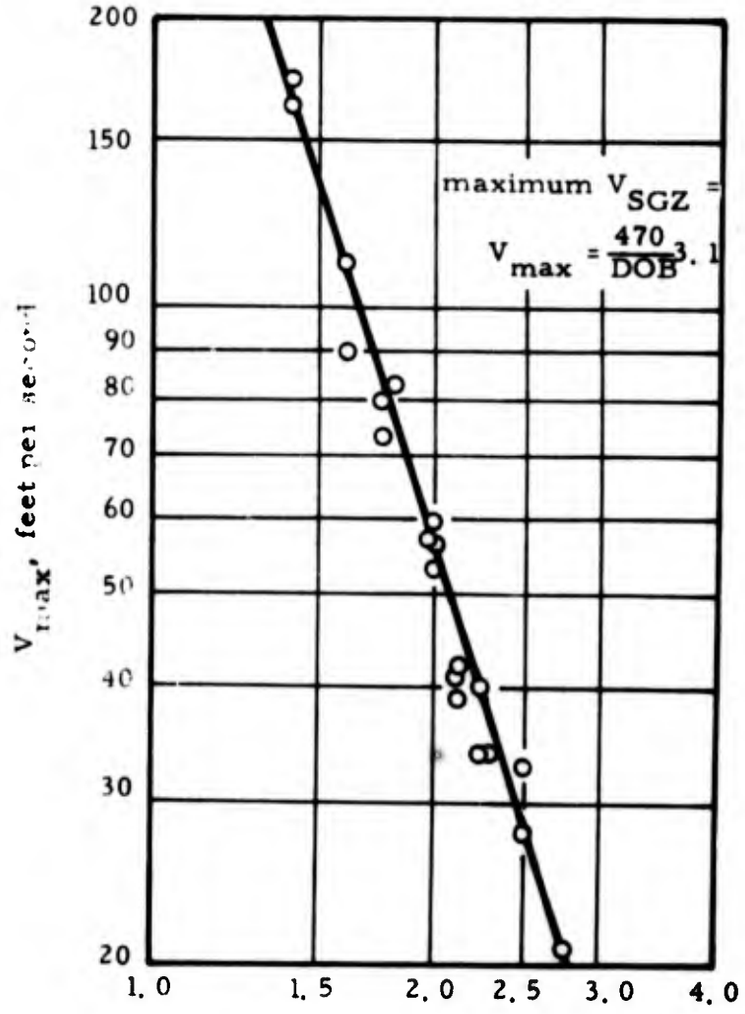

Figure 3.7

4. The push rods slowed to velocities slightly in excess of the surface target velocities within 1 to 3 msec after the initial motion.

5. Motion was essentially vertical for about 0.5 foot of displacement, then the bases were accelerated in the radial direction.

6. The radial velocities were 1.5 to 2 times the surface target velocities until the bases were about 1 foot from the vertical axis through the shotpoint.

3.3 EJECTA STUDIES

The postshot position of the colored sand layers gives a qualitative picture of final sand displacements and deformations. The postshot drawings of the colored sand layers shown in Figures 3.8A through 3.8D were prepared from postshot color photographs taken through a six-inch wire grid.

The final ejecta pellet elevations and their horizontal displacements from SGZ were noted and plotted. The distances of those ejecta pellets which travelled farther than 5 feet from the shot point were measured, and contours of equal throwout displacement for four selected craters are shown in Figures 3.9A (all distances in feet) through 3.9D. The displacement vectors of the pellets in the near vicinity of the crater are also shown in these figures.

ZULU II

Shot SS-19 DOB 1.4 eet

COLORED SAND LAYERS

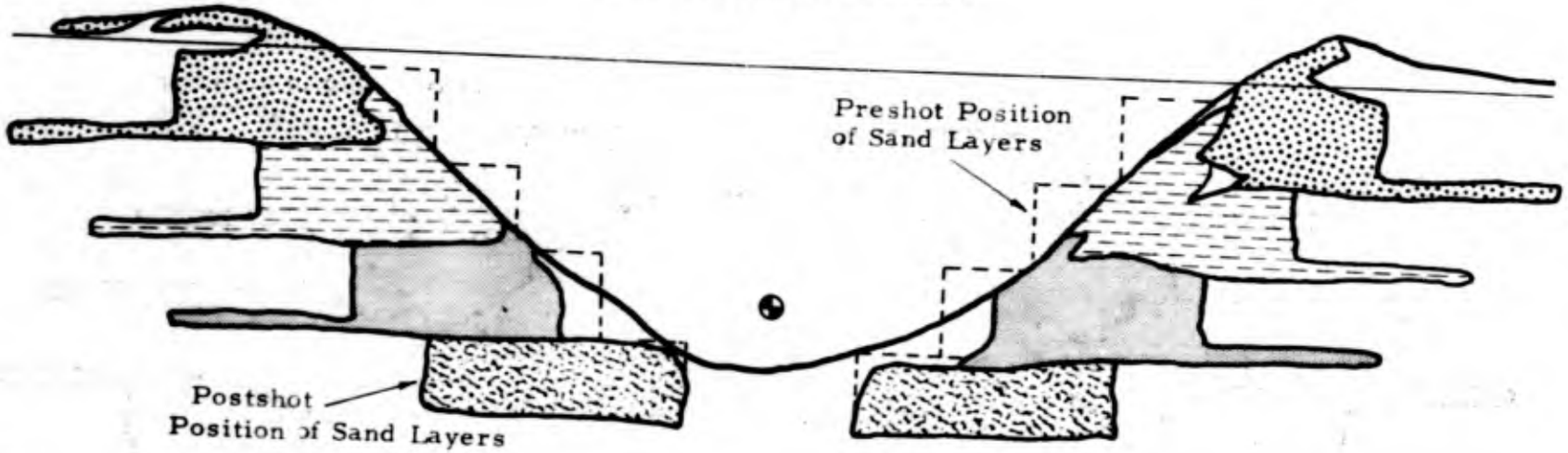

0 1

Scale in Feet

Figure 3.8A

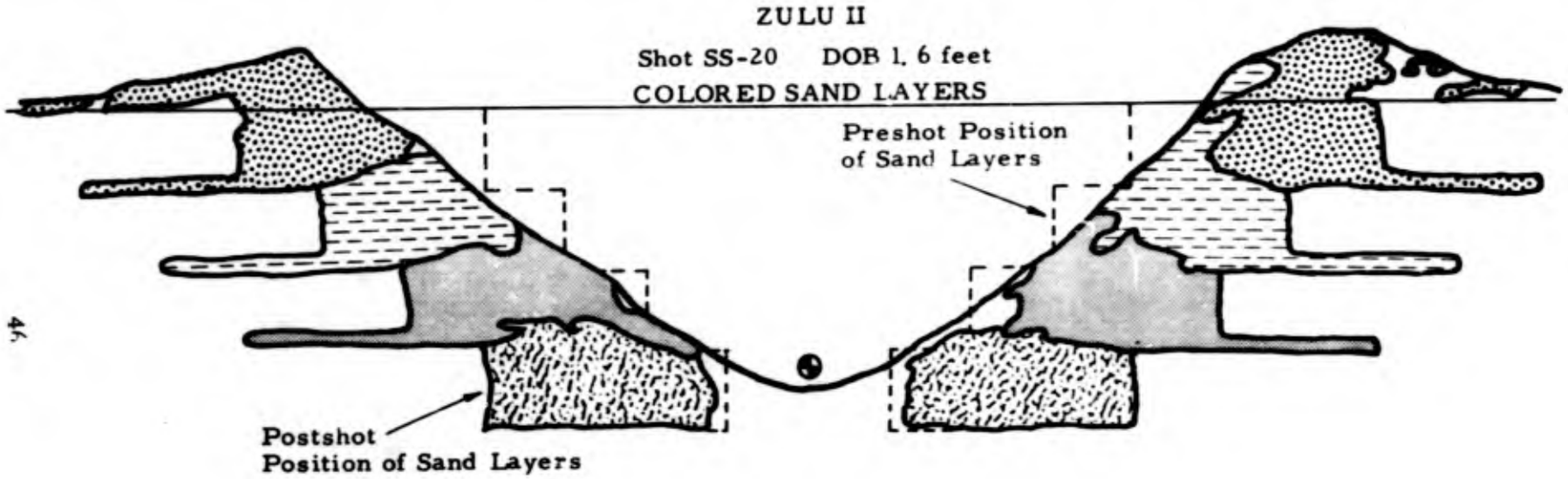
ZULU II
Shot SS-20 DOB 1. 6 feet
COLORED SAND LAYERS
Preshot Position
of Sand Layers
Postshot
Position of Sand Layers
0
1
Scale in Feet

Figure 3.8B

ZULU II

Shot SS-21 DOB 1.8 Feet

COLORED SAND LAYERS

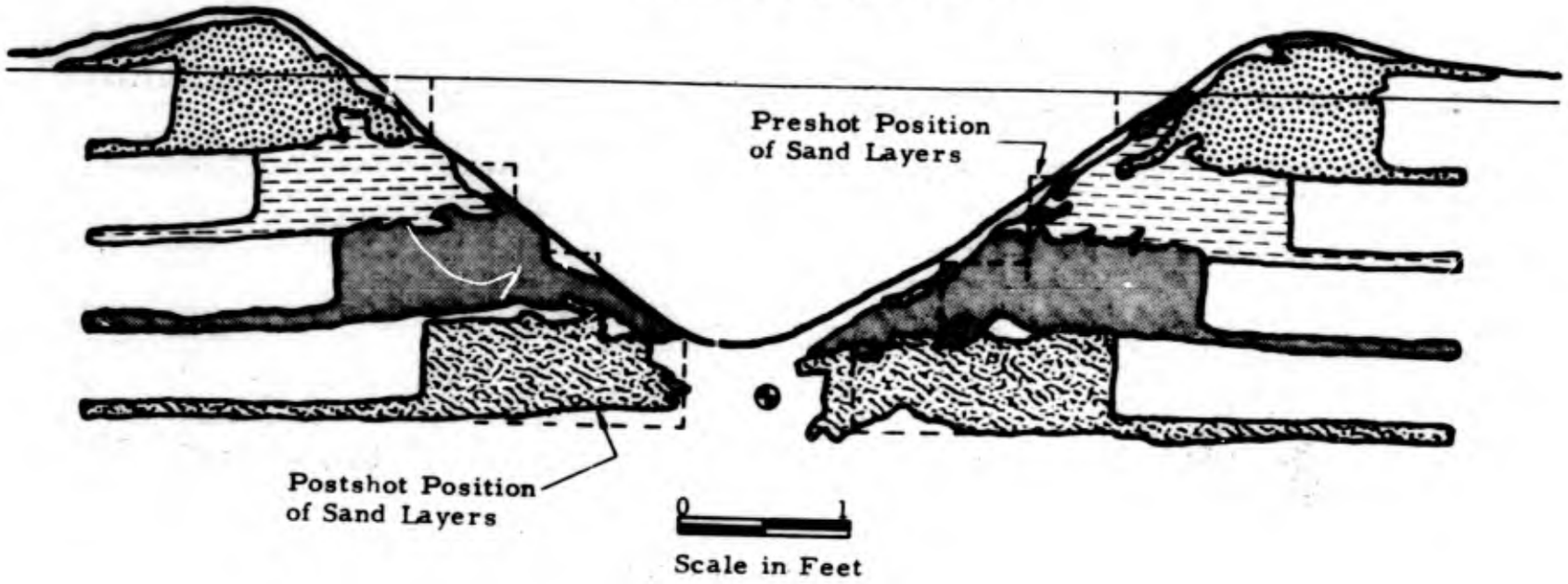

Figure 3.8C

ZULU II

Shot SS-22 DOB 2.0 feet

COLORED SAND LAYERS

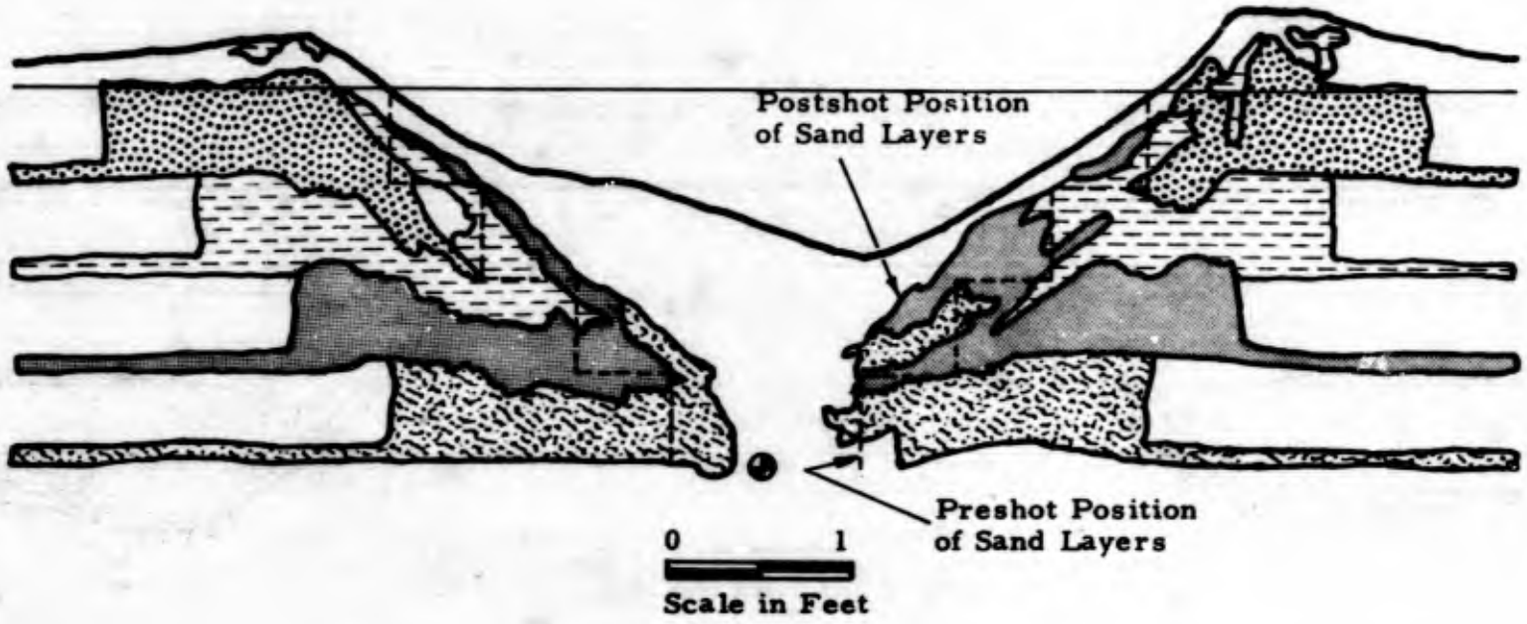

Figure 3.8D

ZULU II

Shot SS-19 DOB 1.4 feet

EJECTA PELLET DISPLACEMENTS
Contour Interval = 10 feet

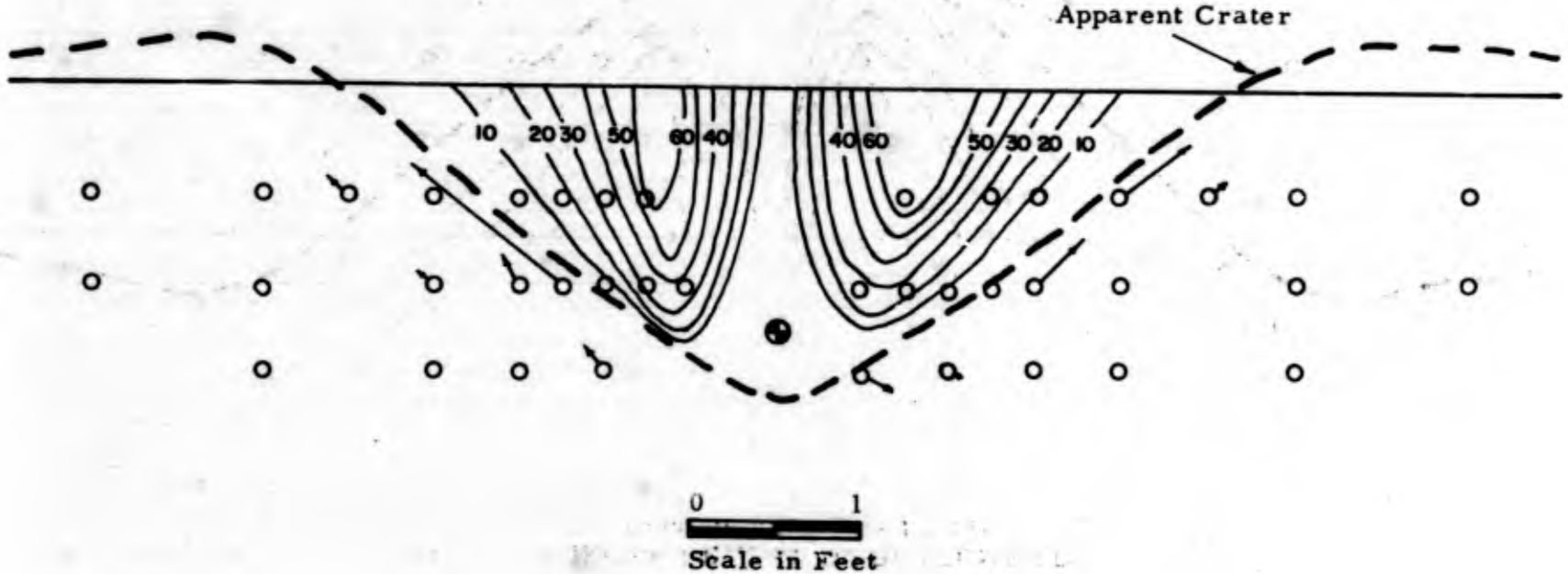

Figure 3.9A

ZULU II

Shot SS-20 DOB 1, 6 feet

EJECTA PELLET DISPLACEMENTS
Contour Interval = 10 feet

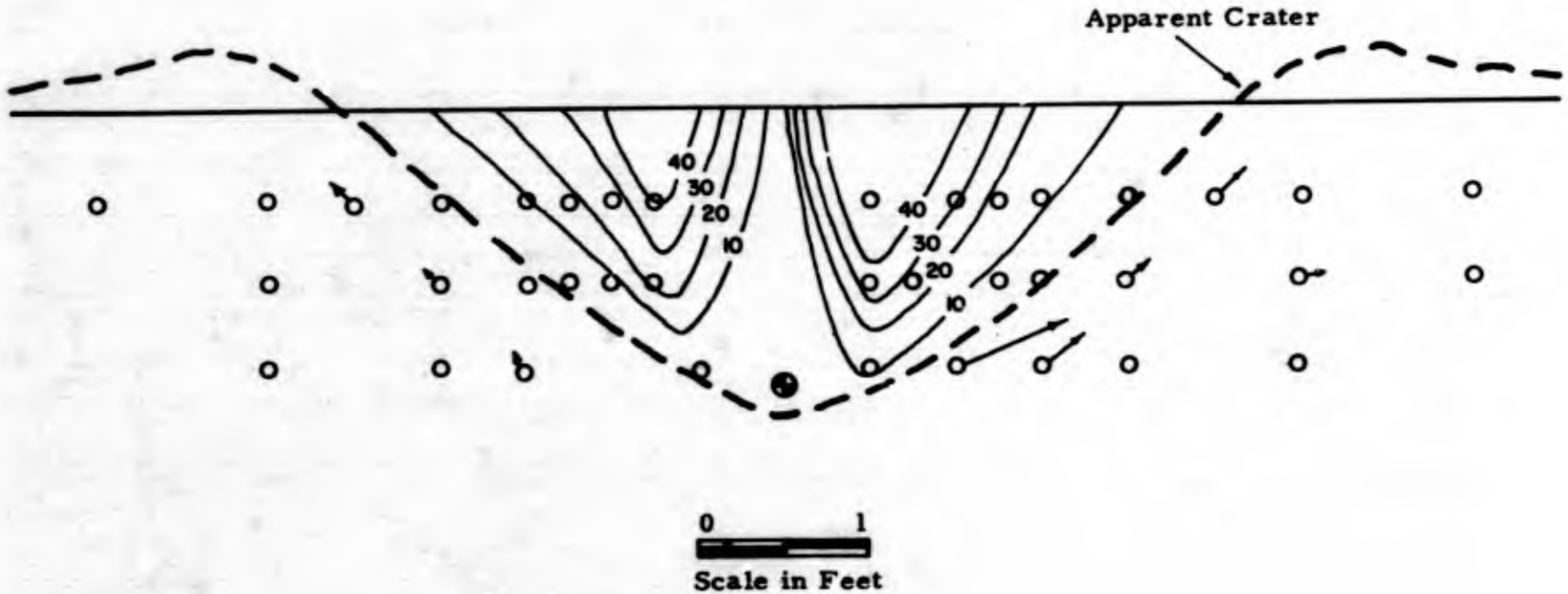

Figure 3.9B

ZULU H

Shot SS-21 DOB 1.8 feet

EJECTA PELLET DISPLACEMENTS

Contour Interval = 10 feet

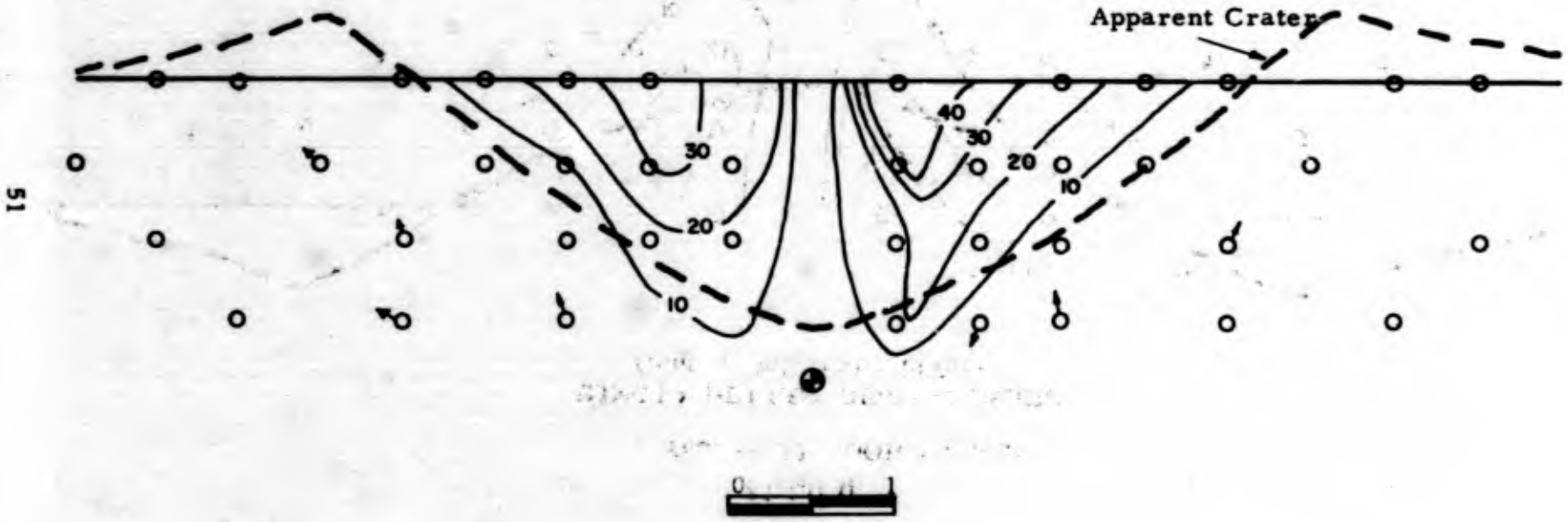

Figure 3.9C

ZULU II

Shot SS-22 DOB 2.0 feet

EJECTA PELLET DISPLACEMENTS
Contour Interval = 10 feet

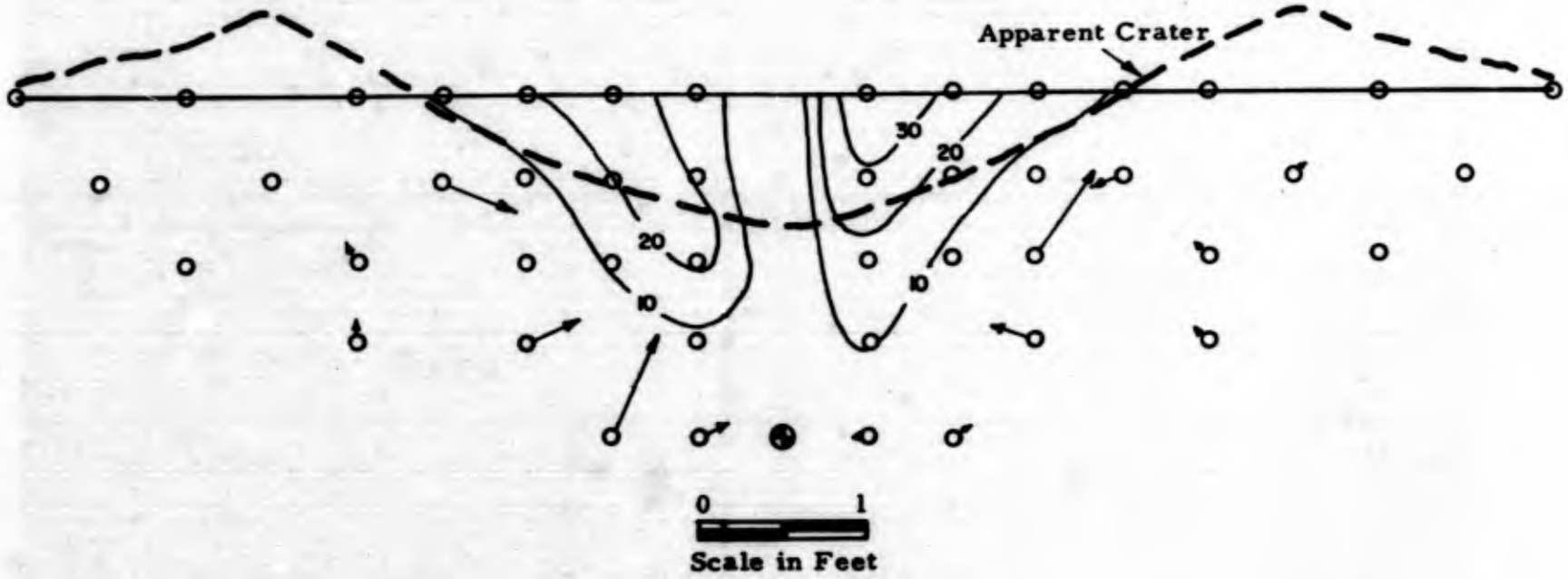

Figure 3.9D

CHAPTER 4

ANALYSIS AND DISCUSSION

4.1 CRATER MEASUREMENTS

The principle objectives of ZULU II cratering program were to determine if reproducible craters could be obtained in a moist, compacted sand and to investigate the cratering characteristics of the medium. Forty-two 1-pound single-charge cratering tests are considered in this report. The results of nine 1/2-pound and six 2-pound shots are presented in Appendix A to illustrate the scaling properties of small charges in a moist sand medium.

Analyses of Figure 3.1 indicates that the reproducibility of crater dimensions at a given DOB is extremely good, except at depths of two feet or greater. The maximum fractional standard deviation from the curve in Figure 3.1 at a depth of two feet is less than 7% in radius and less than 21% in depth.

The crater dimensions obtained from contour maps for DOBs of 0.0, 0.5, 1.0, 1.5, 1.75, and 2.0 feet are also shown on Figure 3.1. These crater dimensions are better averages for the craters and would, therefore, be expected to exhibit less scatter for any given depth of burst, as is suggested by the appropriate points in Figure 3.1. The resulting curves through these points are very similar to those obtained from the surface surveys. The method of obtaining crater measurements from conventional surface surveys is satisfactory considering the inherent scatter in the dimensional data, although a relatively larger number of craters should be measured to obtain a more representative average. A contour map will provide more representative dimensions when analyzing an individual

crater, however, the use of contour maps is more costly and time consuming than surface surveys.

4.2 SURFACE MOTION STUDIES

The usefulness of surface motion data depends on the accuracy with which the target displacements are calculated. Sources of error in the calculation of displacements include the following:

1. Target and reference point reading errors
2. Length and time scaling errors
3. Vibrational motion of the camera
4. Film skew on the microscope platform
5. Incorrect zero time

The target displacements were read to an accuracy of ± 0.02 foot (28 mm lens) and ± 0.01 foot (55 mm lens) using manual displacement determination. An accuracy of ± 0.005 foot was possible with the 28 mm lens and the digitizing microscope.

The performance of the targets varied as a function of the depth of burst. For the deeper shots (below 2 feet), target velocities were within one or two percent of the corresponding mound velocities for major portion of the motion history. For the shallower shots, the targets followed the rising mound velocities well for the first 10 to 15 msec and then were enveloped by the mound. For detonations at 1 foot or less, the targets near SGZ were obscured by venting within a few msec.

The general shape of the vertical velocity history curve ($\dot{y}$ versus time shown in Figure 3.4), was the same for all SGZ targets regardless of DOB. The magnitude of the velocities, however, varied by a factor of three over the range of DOBs from 1.6 feet to 2.1 feet as shown in Figure 3.4. There

are two phases to the vertical and horizontal velocity history curves. The first phase is a rapid acceleration to a peak velocity until the second phase is reached and the material goes into "freefall" or a deceleration of approximately -g. The separate influences of spall and gas acceleration during the first phase of motion (Reference 9) were not resolvable in these experiments because of the short time scale of the cratering phenomenon and the limitation of film speed.

The SGZ target and those targets close to SGZ achieved freefall earlier than targets farther away from SGZ. Therefore, the SGZ targets for the mounds shown in Figures 3.5A - 3.5F were in freefall for some time before the entire mound achieved freefall. The mounds for shallower shots achieved freefall earlier than the deeper shots (1.4- and 1.6-feet DOB-30 msec; 1.8-feet DOB-35 msec; 2.0- and 2.1-feet DOB-45 msec; 2.24-feet DOB-55 msec). However, mounds produced by the shallower detonations were much higher at freefall due to their higher velocities.

The early direction, θ_o, of target velocities shown in Figure 3.6 exhibit the following features:

1. For most detonations, the early directions of motion were symmetrical with respect to the vertical axis of symmetry through the zero point.

2. The angle between the initial direction of motion and the vertical, θ_o, increased with increasing radial angle, θ_r, which is measured between the vertical and a line from the center of the charge to the target's preshot position.

3. θ_o is consistently less than θ_r; and

4. The difference $\theta_r - \theta_o$ was erratic and not subject to quantitative

description as a function of the DOB. As a first approximation the difference was as large as 15 degrees for a θ_r equal to 60 degrees.

Figure 4. 1 shows a log-log coordinate plot of peak resultant and peak vertical target velocities, normalized to the peak SGZ velocity, as a function of the cosine of the radial angle θ_r.

A visual best fit through the resultant velocities is

$$\frac{V}{V_{SGZ}} = \text{Cos}^{3.6}\,\theta_r \qquad 4.1$$

and a similar description of the (normalized) vertical velocities is

$$\frac{\dot{y}}{V_{SGZ}} = \text{Cos}^{6.0}\,\theta_r \qquad 4.2$$

The variation of V_{SGZ} with depth is shown in Figure 3. 7 and is described by

$$V_{SGZ} = 470/\text{DOB}^{3.1} \qquad 4.3$$

Substitution of equation 4. 3 into equations 4. 1 and 4. 2 yields

$$V = 470\left(\frac{\text{Cos}^{3.6}\,\theta_r}{\text{DOB}^{3.1}}\right) \qquad 4.4$$

and

$$\dot{y} = 470\left(\frac{\text{Cos}^{6.0}\,\theta_r}{\text{DOB}^{3.1}}\right) \qquad 4.5$$

Equations 4. 4 and 4. 5 relate the maximum velocity at any point on the ground surface to the depth of burst and radial angle.

Figure 4. 2 shows a linear plot of these same normalized velocities as a function of θ_r rather than Cos θ_r as in Figure 4. 1. Figure 4. 2 could be used for synthesizing the vertical component or surface motion velocities along a row of charges by superposition of the velocity curves for two

A Plot Showing Normalized Target Velocities Compared to Cosine θ_r.

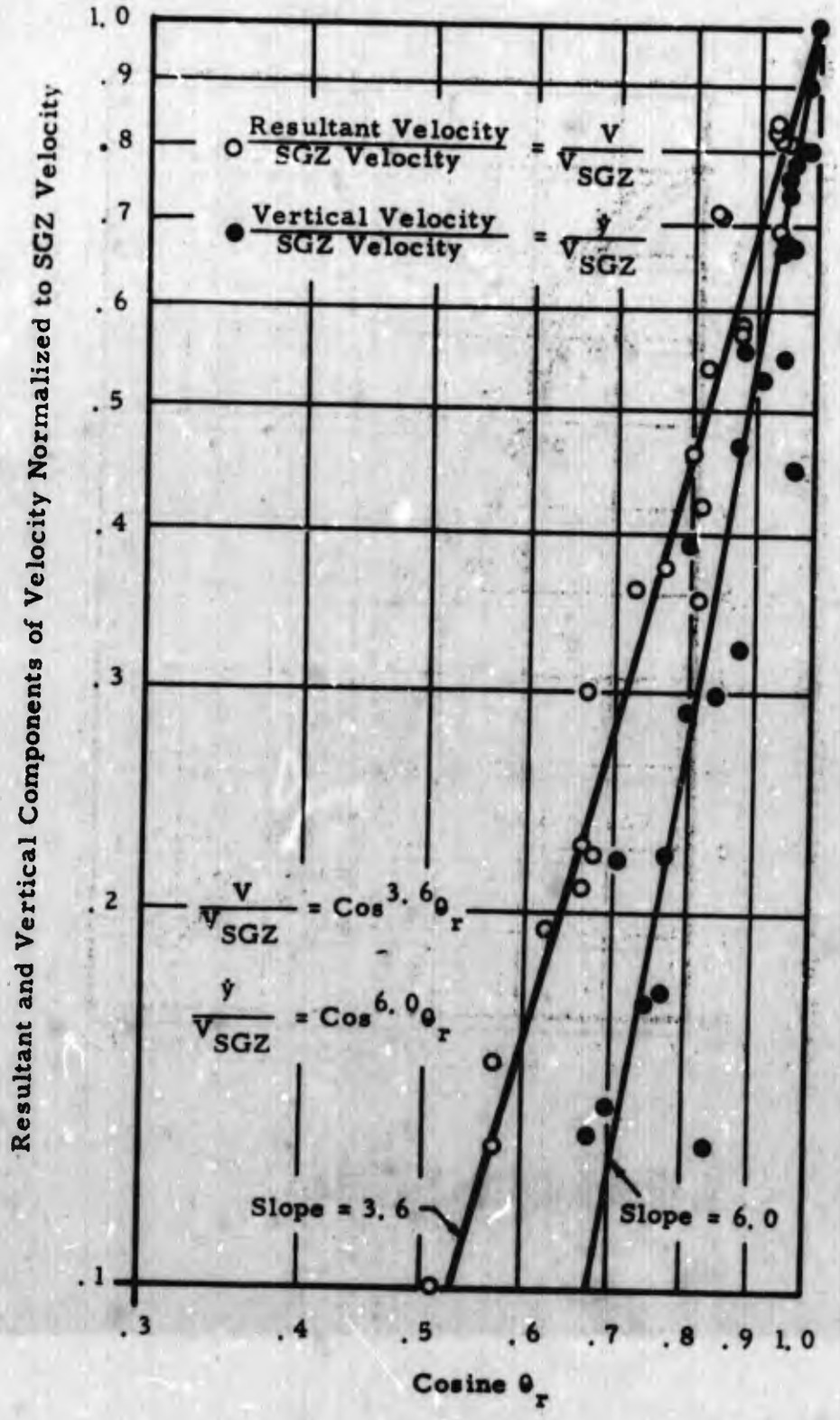

Figure 4.1

A Plot Showing Normalized Target Velocities Compared to θ_r.

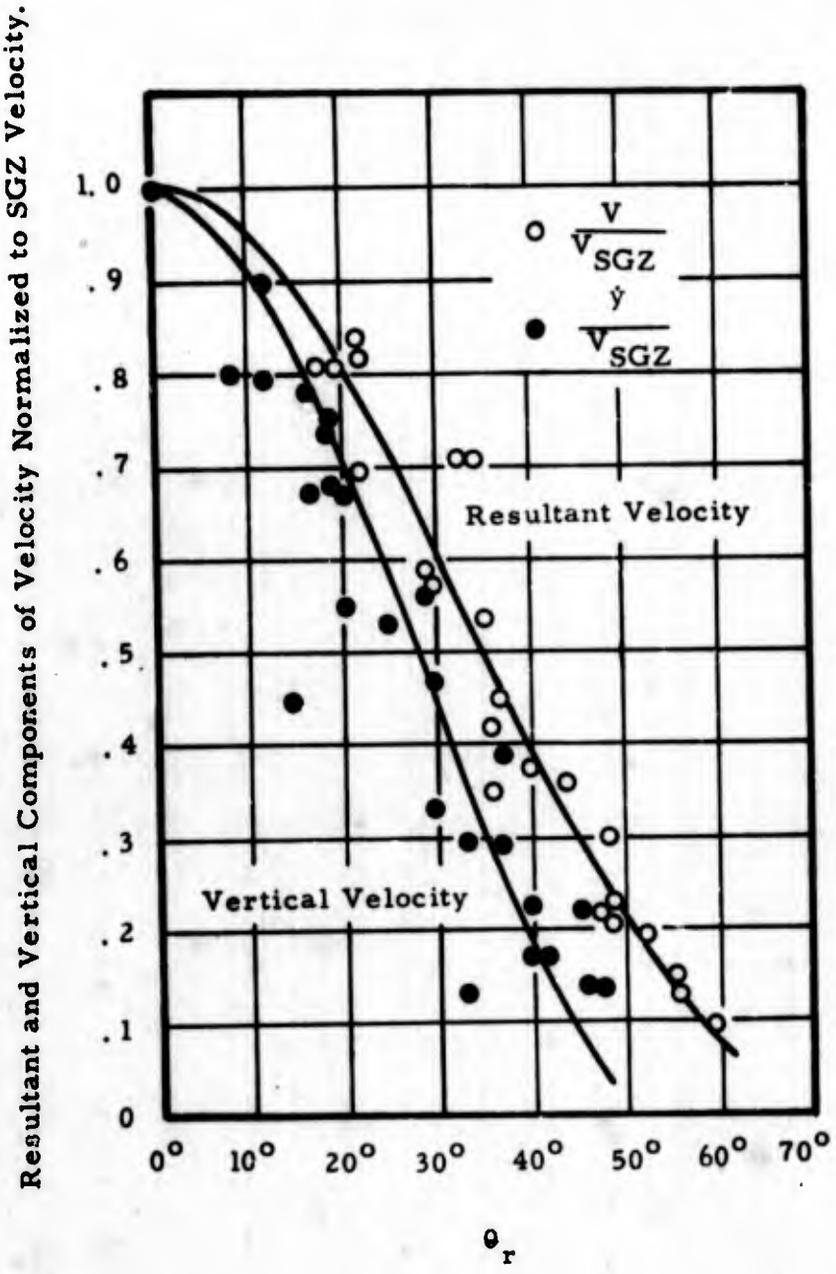

Figure 4.2

adjacent charges. It is probable that the initial motion of the push rod bases and the subsurface material is caused by the passage of the explosive shock front, rather than the expansion of the cavity. Because these high velocities are not observed at the surface, the high subsurface velocities indicated by the push rods must attenuate rapidly with increasing distance from the ZP. Motion of the subsurface material becomes predominantly radial in direction as the mound develops.

4.3 EJECTA STUDIES

The data from both the ejecta pellets and the colored sand layers provided information on both ejected particles and those particles which were merely displaced within the crater.

By noting the final and original positions of the spheres, their trajectories could be approximated. The trajectories of the spheres, as indicated by their final positions, do not represent the displacements of the sand particles. In general, the ejecta pellets travelled farther than the sand particles and the final location of the ejected pellets did not correspond to the final location of the sand particles. This difference probably resulted because the spheres were not affected by interparticle collisions and air drag as were the individual sand particles. Figures 3.9A through 3.9D show that particles located in a vertical column above the shot point travelled the farthest. Although the ejected pellets did not correspond to the ejected sand particles, Figures 3.9A through 3.9D give a qualitative picture of the ejecta mechanism.

Ejecta pellet displacements also produced information about the movements of the material not ejected from the crater. Near the apparent crater boundary, material was displaced inward and downward indicating a

slumping action. Farther away from SGZ, displacements are upward as a result of uplifting and bulking of the surrounding material.

The results of the sphere displacement data were supported by the photographs of the displaced colored sand layers. There was some distortion in the photographs which prohibited an accurate quantitative descriptt-ion. However, the photographs clearly showed sand-layer displacements in the same directions as the displacements noted for the spheres. The disturbed colored sand layers clearly showed the phenomena of foldback of the cratered material to form the lip. They also showed the shearing of the material in the rupture zone and subsequent slumping of the material into the crater. The uplifting of the material surrounding the crater was obvious from the colored sand photographs.

The basic formation of the crater occurs rather quickly and the amount of sand which remains in the air for long periods of time is relatively small. Much of the sand remained in fairly uniform colored clods. This indicates that the sand was not thrown very high and did not break up to a great extent. It was also apparent that the colored material which was thoroughly mixed comprised only a small layer on the surface of the crater except for the deeper shots. This supports the concept that the sand above the deeper shots is thrown upward and mixed but is not ejected outward. A subjective interpretation of the dynamic crater formation process leading to the final crater configuration illustrated by the colored sand layers is presented in reference 5.

CHAPTER 5

SUMMARY AND CONCLUSIONS

5.1 CRATER STUDIES

Crater dimensions were shown to be reasonably reproducible at a given depth of burst except at the deeper DOBs, i.e., 2.0 feet or greater. For charges buried at 2.0 feet, the fractional standard deviation in apparent radius was less than 7% and less than 21% in apparent depth. A few surface surveys are sufficient for defining the crater dimensions within the limits of inherent scatter. The cratering curves developed for the one-pound charges show that an optimum charge DOB of 1.50 feet resulted in a crater which had an R_a of 2.25 feet and a D_a of 1.80 feet. The detonation of additional one-half-pound and two-pound C-4 single charges showed that cube root scaling of apparent crater dimensions was applicable for the charge yields involved.

5.2 SURFACE MOTION STUDIES

The surface motion studies indicated that the maximum resultant velocity of a surface particle could be described by the equation:

$$V = \frac{\text{Cos}^{3.6}\theta_r}{\text{DOB}^{3.1}}$$

As the DOB increased, the velocities over the entire mound decreased. Also, as the DOB increased, the shape of the mound upon achieving freefall changed. For a shallow DOB, the forces of the expanding gas cavity acted upon the material for a sufficient length of time that the mound was high and narrow when it achieved freefall. For a deep DOB, the mound was low and flat upon achieving freefall. The deeper shots did not impart sufficient

lateral velocity to the material to eject it from the crater.

The formation of the crater appeared to depend upon two factors: (1) the peak magnitude velocities over the entire mound, and (2) the height and shape of the mound when it achieved freefall. These two factors were interrelated, but individually important. If the particles did not achieve sufficient velocities and the mound was not of sufficient height at the end of the acceleration phase, the material was not ejected from the crater.

The subsurface material, especially for deeper shots, did not move radially outward from the shot point. Its movement was more vertical. It is also evident that the movement of the surface particles for these deeper shots was not necessarily indicative of the movement of the subsurface particles.

5.3 EJECTA STUDIES

The ejecta pellet studies indicated that the pellets did not accurately describe the movement of the ejected sand material during crater formation. Analysis of the ejecta pellets displacement data indicated that the fallback was composed primarily of material which was originally either directly over the zero point or in close proximity to the apparent crater boundary.

REFERENCES

1. B. C. Hughes and R. H. Benfer; "Project ZULU" a One-Pound High Explosive Cratering Experiment in Scalped and Remolded Desert Alluvium"; NCG/TM 65-9; U. S. Army Engineer Nuclear Cratering Group, Livermore, California.

2. "Report of Soil Tests on Cratering Materials for Site 300"; U. S. Army Engineer Division Laboratory, South Pacific; Corps of Engineers, Sausilito, California; May 1966.

3. K. L. Larner; "Phase I, Project ZULU II"; unpublished draft; U. S. Army Engineer Nuclear Cratering Group, Livermore, California.

4. W. G. Christopher; "Analysis of Surface Motion Phenomena of One-Pound ZULU II Charges of Varying Depth of Bursts"; (NCG/TM 66-14) U. S. Army Engineer Nuclear Cratering Group, Livermore, California; 1966.

5. R. G. Bening and M. K. Kurtz; "The Formation of a Crater as Observed in a Series of Laboratory-Scale Cratering Experiments"; PNE 5011; U. S. Army Engineer Nuclear Cratering Group, Livermore, California; 1967.

6. Roger H. Paul and Joseph L. Spruill; "Project Pre-SCHOONER, Crater Measurements"; PNE 502F; U. S. Army Engineer Nuclear Cratering Group, Livermore, California; 1965.

7. W. G. Christopher; "Analysis of the Phenomena Within the Immediate Crater Area Resulting from the Detonation of One-Pound ZULU II Charges", NCG/TM 66-15; U. S. Army Engineer Nuclear Cratering Group, Livermore, California.

8. W. R. Perret, A. J. Chabai, J. W. Reed, and L. J. Vortman, "Project

SCOOTER," SC-4602(RR), TID-4500, Sandia Corporation, Albuquerque, N. M.; October, 1963.

9. E. Teller, W. Talley, G. Higgins and G. Johnson; "The Constructive Uses of Nuclear Explosives," p 142; McGraw Hill, N. Y., N. Y.

APPENDIX A: SCALING PROPERTIES OF THE ZUNI II SAND

The data from nine experiments conducted at the half-pound level and six experiments at the two-pound level (See Table A. 1) are included in this report to demonstrate the variation in crater size with different charge weights. Assuming that crater dimensions are a function of the ratio of charge weights raised to some power, then

$$\frac{R_2}{R_1} = \frac{D_2}{D_1} = \frac{Z_2}{Z_1} = \left(\frac{W_2}{W_1}\right)^P$$

where R = radius of apparent crater

D = depth of apparent crater

Z = depth to shot point

W = weight of charge

P = exponent determined from data

The cratering curves for the various charge weights are shown in Figure A. 1. If the function stated above applies, then the ratios of points intersected by a line drawn through the origin and passing through two cratering curves will remain constant for any line drawn in a similar manner. The following example illustrates this principle.

A line is drawn as shown in Figure A. 1 and from this we can see that $\frac{R_2}{R_1} = \frac{Z_2}{Z_1}$. By inserting the values: R_2 (radius for 2-pound charge = 3. 12 feet)

and R_1 (radius for 1-pound charge = 2. 48 feet)

$$\left(\frac{3.12}{2.48}\right) = \frac{R_2}{R_1} = \left(\frac{W_2}{W_1}\right)^P = \left(\frac{2}{1}\right)^P = 1.26$$

$$\log 1.26 = P \log 2$$

$$P = \frac{\log 1.26}{\log 2} = \frac{0.10}{0.301} = \frac{1}{3}$$

By performing this exercise with a number of radial lines, it was found that

TABLE A. 1

SUMMARY OF RESULTS FOR SINGLE CHARGE CRATERS

Two-Pound C-4 Spheres

DOB	Shot No.	D_a	R_a	H_{al}	R_{al}	Dry Density
feet		feet	feet	feet	feet	pcf
0. 60	26	1. 30	2. 78	0. 25	3. 38	112. 3
1. 25	22	2. 00	3. 20	0. 32	4. 00	111. 2
1. 60	29	2. 40	3. 30	0. 40	4. 20	112. 3
2. 00	20	2. 10	3. 30	0. 50	4. 38	112. 1
2. 25	25	1. 78	3. 25	0. 32	4. 00	111. 2
2. 50	21	1. 00	2. 78	0. 57	3. 80	112. 1

One half-Pound C-4 Spheres

DOB	Shot No.	D_a	R_a	H_{al}	R_{al}	Dry Density
feet		feet	feet	feet	feet	pcf
0. 00	34	0. 35	1. 22	0. 10	1. 90	112. 9
0. 50	30	0. 95	1. 85	0. 20	2. 25	112. 9
0. 75	27	1. 15	2. 00	0. 18	2. 25	112. 3
1. 00	23	1. 45	2. 13	0. 15	2. 88	111. 2
1. 15	32	1. 45	2. 13	0. 27	2. 20	112. 9
1. 25	28	1. 55	2. 15	0. 20	2. 13	112. 3
1. 35	33	1. 55	2. 10	0. 30	2. 75	112. 9
1. 50	24	1. 35	2. 12	0. 26	2. 15	111. 2
1. 60	31	1. 15	2. 00	0. 35	2. 80	112. 9

Cratering Curves Used to Determine the Scaling Relationship Among 1/2-, 1-, and 2-pound Single Charge Craters.

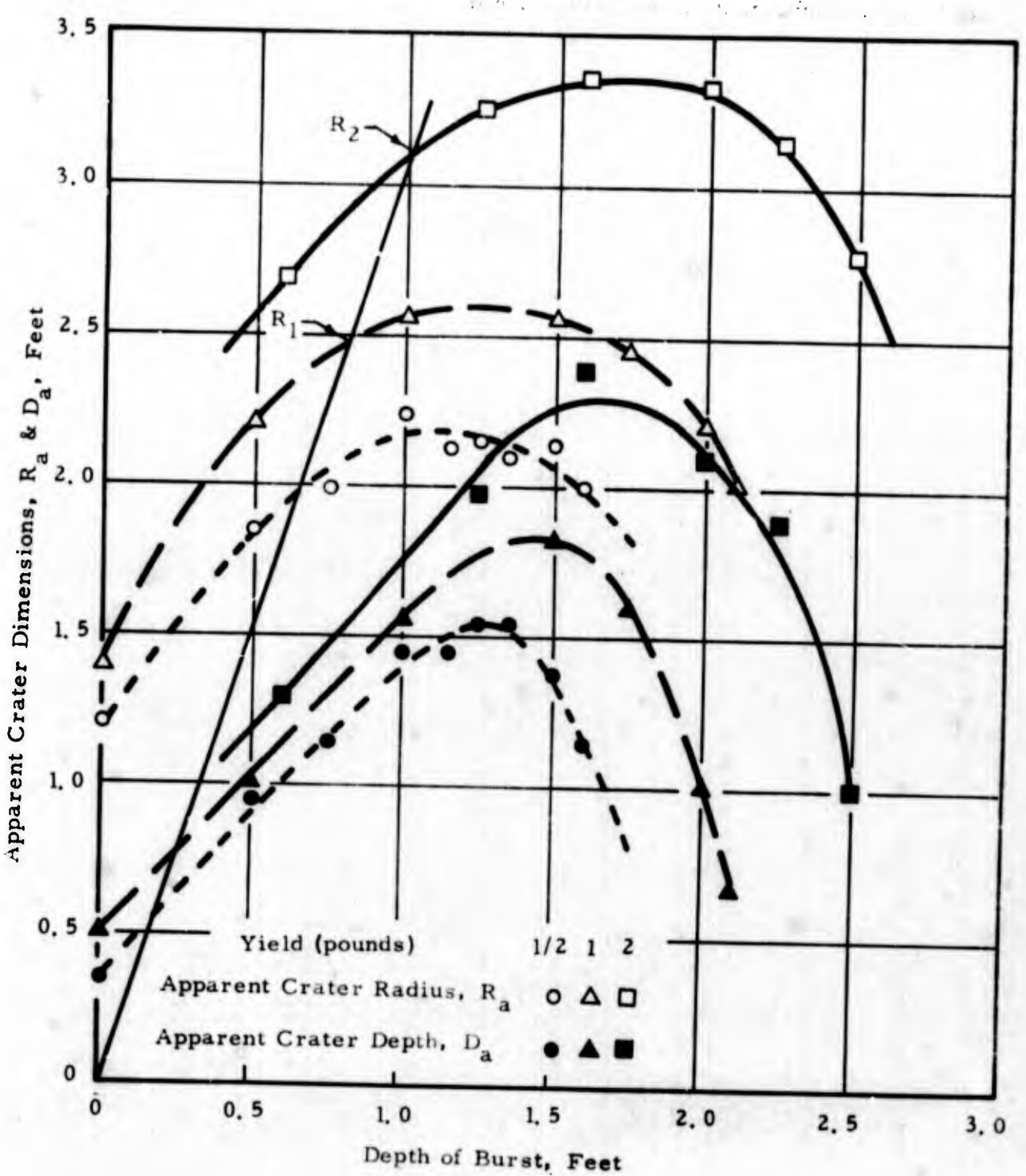

the value of P averaged 1/3. This indicates that crater measurements scale as the cube root of the charge yield.

Unclassified
Security Classification

DOCUMENT CONTROL DATA - R & D

(Security classification of title, body of abstract and indexing annotation must be entered when the overall report is classified)

1. ORIGINATING ACTIVITY (Corporate author) US Army Engineer Nuclear Cratering Group Lawrence Radiation Laboratory Livermore, California 94550	2a. REPORT SECURITY CLASSIFICATION Unclassified 2b. GROUP

3. REPORT TITLE

PROJECT ZULU II - PHASE I

SINGLE-CHARGE CALIBRATION SERIES

4. DESCRIPTIVE NOTES (Type of report and inclusive dates)

Final Report

5. AUTHOR(S) (First name, middle initial, last name)

SP4 W. W. Johnson and 1LT D. L. Nelson

6. REPORT DATE	7a. TOTAL NO. OF PAGES	7b. NO. OF REFS
November 1968	75	9

8a. CONTRACT OR GRANT NO. b. PROJECT NO. c. d.	9a. ORIGINATOR'S REPORT NUMBER(S) Technical Report No. 3 9b. OTHER REPORT NO(S) (Any other numbers that may be assigned this report) AD

10. DISTRIBUTION STATEMENT

Distribution of this report is unlimited.

11. SUPPLEMENTARY NOTES	12. SPONSORING MILITARY ACTIVITY
N/A	N/A

13. ABSTRACT

Phase I of Project ZULU II was a laboratory-scale crater modeling experimental series consisting of the detonation of forty-two 1-pound C-4 charges in a moist compacted sand. This experimental series was conducted by the U.S. Army Engineer Nuclear Cratering Group (NCG) at the University of California Lawrence Radiation Laboratory's (LRL) High Explosive Test Facility, Site 300, near Livermore, California.

The primary objectives of Phase I of Project ZULU II were: (1) to calibrate the medium with respect to its cratering characteristics; (2) to determine the reproducibility of the crater dimensions; (3) to conduct surface motion studies; and (4) to study ejecta and fallback distribution as well as the nature of the displacements occurring in the near vicinity of the zero point and the rupture zone.

The cratering curves developed from these experimental series showed an optimum depth of burst (DOB) of 1.5 feet and a rapid decrease of apparent crater dimensions until no crater resulted at a DOB greater than approximately 2.1 feet. The data for ten charges detonated at a nominal DOB of two feet resulted in a fractional standard deviation of 6.4% for crater radius and 20.6% for crater depth, the largest deviations observed for any DOB. The detonation of additional one-half-pound and two-pound C-4 single charges showed that cube-root scaling of apparent crater dimensions was applicable at these yields.

The maximum surface ground zero (SGZ) vertical target velocity, V_{SGZ}, was observed to be a function of DOB and conformed to the relationship $V_{SGZ} = 470/DOB^{3.1}$. The resultant velocity, V, of a surface target can be described in

DD FORM 1 NOV 68 1473

Unclassified
Security Classification

14 KEY WORDS	LINK A		LINK B		LINK C	
	ROLE	WT	ROLE	WT	ROLE	WT

13. ABSTRACT

terms of DOB and the cosine of the angle between the vertical and a line drawn through the surface target and the shot point, θ_r. This equation can be expressed as:

$$V = \frac{470 \cos^{3.6}_{r}}{DOB^{3.1}}$$

The ejecta pellet studies did not successfully record pre- and postshot locations of the material actually ejected from the crater. It was indicated that the fallback was composed of material originating from over the zero point and in the region near the apparent crater boundary.